FACULTY OF TECHNOLOGY

EFFECT OF DETONATOR POSITION ON FRAGMENTATION AT KEVITSA OPEN PIT MINE

Riika Ylitalo

MINING ENGINEERING AND MINERAL PROCESSING

Master's thesis

April 2020

ABSTRACT

Effect of Detonator Position on Fragmentation at Kevitsa Open Pit Mine

Riika Ylitalo

University of Oulu, Mining Engineering and Mineral Processing

Master's thesis 2020, 61 p. + 6 appendices

Supervisor at the university: Zong-Xian Zhang

Blasting is one of the main operations in open pit mining and effective rock blasting can have a major impact on the overall economy of the mine. To obtain optimal rock fragmentation by blasting, explosive energy must be well-utilized, well-distributed, and targeted to the rock mass that we aim to fragment. A position of a detonator in a blasthole affects all of the above.

The aim of this thesis was to study the effect of detonator position on fragmentation at the Kevitsa open pit mine. The theoretical optimum for the detonator position in the explosive column was defined and tested in practice. In addition, the effects on bench floor conditions were investigated.

The practical study consisted of blasted test fields within production blasts, where the current blasting practice used in Kevitsa was compared to the test design representing the theoretical optimum. The effects were measured and studied with shovel-mounted machine vision cameras, test drillings, and loading machine operator feedback forms.

Considering optimal fragmentation and less damage below the bench floor level, both theoretical and field studies indicated that the detonator position plays an important role in rock fragmentation, and that the detonator position in the middle of the explosive column allows for significant improvement in rock fragmentation and bench floor conditions. The results of this study can be applied more generally in open pit blasting.

Keywords: Open pit blasting, Detonator position, Fragmentation, Stress waves

FOREWORD

The research presented in this thesis was carried out during October 2019 to March 2020 at the New Boliden Kevitsa mine in Sodankylä. I am very grateful to the New Boliden, which founded a very interesting research project on the effective blasting of rock.

I would like to thank my supervisor Professor Zong-Xian Zhang for all the important knowledge that he has taught to me and for guiding my thesis; it has been a privilege to learn from him. Thanks to my supervisor M.Sc. Pekka Bergström at the Kevitsa mine for making sure everything works and organizing all the practical help to conduct my work. Thanks to M.Sc. Jouko Salonen for reading and commenting on my thesis. Many thanks also to my other colleagues at the New Boliden Kevitsa and explosive company Orica for supporting, assisting and sharing the expertise during the project.

Last but not least, thanks to my big family, including Mika, Siina, Eeli, my parents, in-laws, Uula, Anna, Enna, Suvi, and my friends who have been supportive, helpful and flexible throughout my eight years of study and work.

Sattanen, 26.03.2020

Riika Ylitalo

TABLE OF CONTENTS

LIST OF ABBREVIATIONS

c_{st}	P-wave velocity in stemming
c_p	P-wave velocity
E	Young's modulus
K_{IC}	Mode I fracture toughness
L	explosive column length
L_{max}	maximum distance from detonator to end of the explosive column
L_{st}	stemming length
m	constant
q	powder factor
SHPB	Split-Hopkinson pressure bar
T_D	detonation time
T_{st}	stress wave travel time in stemming
UCS	uniaxial compressive strength
VOD	velocity of detonation
Z	characteristic impedance

ρ	density
σ	stress
σ_c	compressive stress
σ_s	shear stress
σ_t	tensile stress
v	Poisson's ratio
Ø	blasthole diameter
$Ø_{st}$	stemming material size

1 INTRODUCTION

The current state of rock blasting is that experience-dominant designs and various kinds of empirical formulas are used, leading to non-optimal blasting results. Those empirical designs may be proper enough to achieve a satisfactory results, but not sufficient for optimum results. Scientific design has the potential to significantly improve rock blasting (Zhang 2016). For example, an optimum blast design helps to produce required fragmentation, muckpile looseness and toe conditions, to increase ore recovery and safety, and to reduce costs, explosive wastage and harm to the environment (Bergström 2017; Zhang 2019).

Blasting is one of the main operations in open pit mining and the most economical method to break rock masses. The main purpose of rock blasting is to fracture and move the rock mass so that it can be loaded, hauled and further processed easily and efficiently. The size of the rock fragments produced by blasting has a major impact on the overall economy of the mine; drill and blast costs directly impact on rock fragmentation, which directly impacts the cost of loading, secondary blasting and comminution. Improved fragmentation can reduce mining costs, improve metal recovery, reduce energy consumption, improve mining safety and decrease negative effect on the environment. There are numerous parameters that effect rock fragmentation in open pit mining (Chen et al. 2018; Prasad et al. 2017; Petropoulos et al. 2014; Bergman 2005). The objective of this thesis is to study effect of detonator position on fragmentation at the Kevitsa mine.

The Kevitsa mine is an open pit nickel-copper mine situated in the middle of Finnish Lapland in the municipality of Sodankylä. The deposit was originally discovered in 1987 and the mine has been operating since 2012. Swedish mining and smelting company Boliden acquired the mine in June 2016. The mine produced 7.7 Mt of ore containing nickel, copper, gold, platinum and palladium in 2019. The total mining volume was 39.9 Mt, of which 32.2 Mt (81%) was waste rock.

The position of a detonator in a blasthole plays an important role in the rock fracture and fragmentation, and in ore recovery (Brunton et al. 2010, Menacer et al. 2015, Zhang 2005). This important role has not been well understood so far. Consequently, an improper detonator position can often be found in present open pit blasting. An improper

placement can lead to wastage of detonation energy and non-optimal stress distribution in the rock mass, resulting in poor fragmentation (Zhang 2014; Zhang 2016).

In this thesis, the effect of detonator position is studied theoretically and in practice by choosing optimum detonator position according to blasting theory (stress wave theory) and comparing it with current blasting practice used in Kevitsa. Test blasts are conducted within production blasts by charging one part of the blast field with test design and other part with current practice. Effects on fragment size and size distribution are measured with shovel-mounted machine vision cameras; bench floor conditions, toes, floor humps, boulders, and muckpile diggability are monitored through loading machine operator feedback forms; and the thickness of the loose rock layer formed below the blasted field by test drillings. The expected results are smaller fragment sizes, less boulders, and thinner loose rock layer with the optimum detonator position.

A higher rock amphibole content is expected to result in a worse fragmentation i.e. larger fragment size in the blasting process in Kevitsa. A clear correlation between the two has been observed in the enrichment process, especially in grinding. In this thesis, Split-Hopkinson Pressure Bar (SHPB) tests are conducted to determine the correlation of the dynamic rock strength and amphibole content, and old fragment size data is analyzed to determine the correlation of the fragment size and amphibole content in blasting.

2 THEORETICAL BACKGROUND

Although blasting science has been initiated for several decades ago by many pioneers such as Langefors and Kihlström (1963) up till now rock blasting has been dominated by empirical designs that are not optimal for rock fracture and fragmentation (Zhang 2019). The prevailing notion has been that rock fracture and fragmentation are based on gas expansion in the borehole. Today, however, it is quite well known that fragmentation is mainly due to blast-induced stress waves travelling through the rock mass, without neglecting the effects of gas expansion.

Unlike gases acting on the rock, stress waves can be easily measured and modeled, making it possible to scientifically design an optimal rock blasting using stress wave theory. Given the diverse nature of field conditions, it is unlikely that a universal physical model will ever be developed for all blasting to predict fragmentation (Menacer et al. 2015), but it has been shown that fundamental theory of stress waves and an understanding of dynamic rock fracture allows significant improvement in rock blasting (Zhang 2005).

Rock fragmentation depends mainly on total energy used in fragmentation and stress distribution in the rock mass (Zhang 2016). The size distribution of fragments is important factor for determination of efficiency of blasting. The sizes of the fragments produced by blasting should be small so that loading can be carried out efficiently. An optimum fragmentation also means that the oversize boulders and toes produced are as few as possible and the cost from blasting to grinding is a minimum (Zhang 2005; Bergström 2017). From the practical standpoint, oversize may be defined as a size, which needs secondary fragmentation before further handling. The presence of oversize boulders causes not only loss in production, but also increases the cost and lower the efficiency of loading and comminution operations (Singh & Narendrula 2010).

The controllable parameters effecting on the rock fragmentation include:

- Explosives (e.g. velocity of detonation, density, energy, match between explosive and rock, and powder factor)
- Initiators (e.g. type and quality of detonators)

- Drill plan (e.g. burden, spacing, blast pattern, height of the bench, length and diameter of the blasthole, and subdrilling)
- Blast plan (e.g. detonator placement, length and materials of the stemming, delay time, firing pattern, etc.)

The non-controllable parameters are geological properties like joints, fissures, voids, and dips, density, sonic velocity and strength of the rock, local stress field and confinement etc. (Prasad et al. 2017; Zhang 2016).

2.1 Energy efficiency in mining and blasting

Mining energy consumption contributes to mining operational costs and occurs at all stages of the ore recovery process: drilling, blasting, secondary blasting, loading, hauling, crushing, and grinding. The total energy costs in mining are high. Comminution (crushing and grinding) is the largest and least energy efficient unit operation in mining with 3% energy utilization at the maximum. It uses a more than 50% of a mine's energy consumption, in average, and at least 3% of total global electricity production. Blasting is usually the most energy efficient unit operation with approximately 5-15% energy utilization and explosives are not only powerful but also cheap, as compared to many other types of energy. Therefore, blasting is the most cost and energy efficient way to break rock in mining. Mining business can create significant increases in the Net Present Value (NPV) by applying increased energy to rock breakage and surface area creation through blasting designs (Zhang 2008; Jeswiet & Szekeres 2016; Zhang 2017; Howe & Pan 2018; Boylston 2018; Awuah-Offei 2018; Zhang 2019; Silva et al. 2019).

Explosives can rapidly produce an extremely high pressure and release a huge amount of energy at a moment. In blasting, all energy used in rock fracture and fragmentation comes from the explosive, and the total energy consumed is an important factor in fragmentation. In general, the energy used in blasting can be increased by increasing the amount of explosive charge i.e. powder factor (Zhang 2014; Zhang 2016; Zhang 2019). However, there are also several ways to increase the energy efficiency of blasting. In order to do that, the borehole pressure can be properly increased and pressure losses minimized. This can be achieved for example by:

- Reducing or avoiding detonation energy wastage from the collars by proper stemming and / or by correct detonator placement.
- Increasing the borehole pressure by placing two detonators with same delay time at different positions in a hole to obtain shock wave collision.
- Choosing a proper explosive whose velocity of detonation (VOD) well matches the P-wave velocity of rock mass. Higher VOD corresponds to a higher detonation pressure.

Other ways to increase the energy efficiency are an appropriate delay time to achieve effective stress superposition between holes, or use kinetic energy of flying fragments for secondary fragmentation (Zhang 2017; Konya & Konya 2018).

2.2 Important rock / rock mass properties

The most important rock properties that affect blasting are rock strength, fracture toughness and rock mass structure. Rock masses consist of intact rock and discontinuities, and discontinuities within the rock masses greatly influence their strengths. The discontinuities such as joints have a large impact on rock fragmentation in bench blasting (Bergman 2005; Beyglou et al. 2015). The majority of pressure losses in blasting occur from premature borehole venting and through weak layers intersecting the borehole (Konya & Konya). Geology is a major contributor to the formation of boulders (Singh & Narendrula 2010). A careful adaptation of blast design to existing discontinuities could result in significant improvement in fragmentation and therefore save the production costs (Orica 1998; USDA 2012; Yi et al. 2019).

2.2.1 Rock strength

The strength of a material is its ability to withstand an applied load without failure or plastic deformation. The common rock strengths are compressive σ_c, tensile σ_t, and shear strength σ_s presented in Figure 1, where F represents the external force and A is the cross-sectional area of the rock specimen.

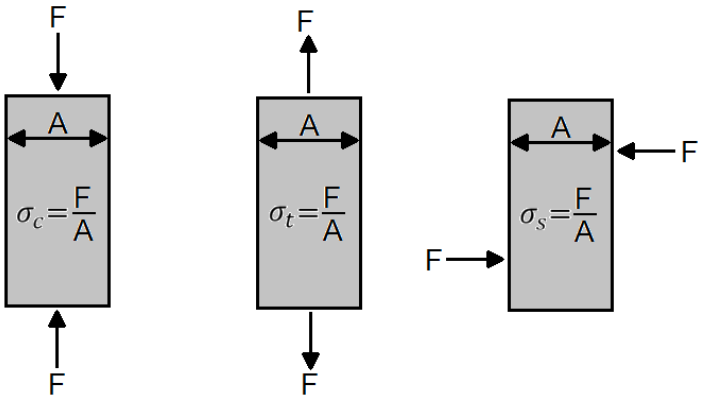

Figure 1. Compressive σ_c, tensile σ_t, and shear σ_s strength of rock.

The tensile strength of a rock are often less than their shear strength and much smaller than compressive strength. The strength relation in rocks can be expressed by simple formula:

$$\sigma_t < \sigma_s \ll \sigma_c \tag{1}$$

Commonly the compressive strength is 8-15 times the tensile strength, with an average of 10 (Read J. & Stacey 2009; Zhang 2016). It is a well-known fact that a tensile stress is very important in making rock fracture and fragmentation (Orica 1998; Zhang 2005; Menacer et al. 2015).

Fracture toughness refers to the resistance of a material to crack extension (Zhang 2016). The Mode I fracture toughness K_{IC} and the tensile strength of rock are well related to each other; an empirical relation between them is (Zhang 2002):

$$\sigma_t = 6.88\, K_{IC} \tag{2}$$

Under dynamic loading condition such as blasting, compressive strength, tensile strength, shear strength, and Mode I fracture toughness of a rock increases with an increasing loading rate. As shown in Figure 2, fracture toughness increases rapidly with increasing loading rate under dynamic loading, while under static loading the fracture toughness varies very little. Despite the fact that rock strength increases, the sizes of rock fragments markedly decrease with increasing loading rates (Zhang 2016).

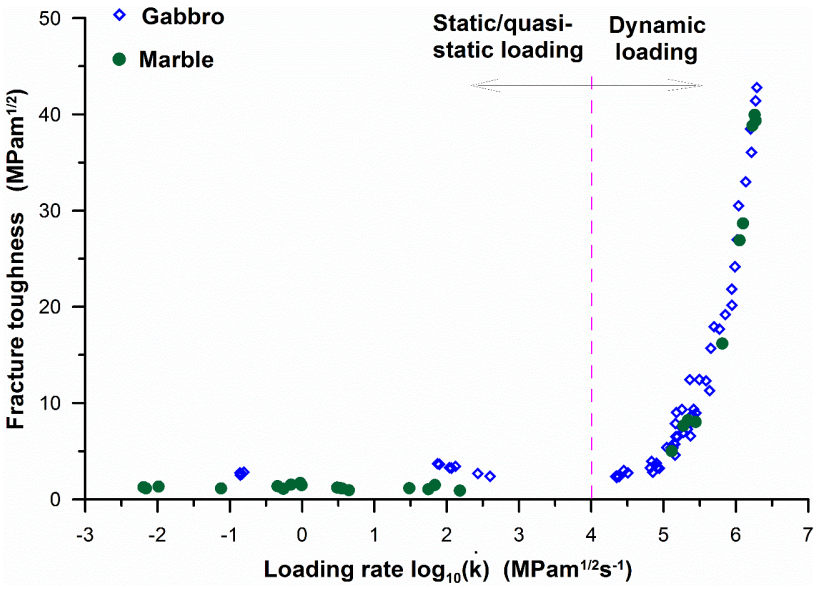

Figure 2. Fracture toughness versus loading rate (Zhang 2016).

The laboratory-measured Uniaxial Compressive Strength (UCS) is the standard strength parameter of intact rock material. The dynamic rock strength can be determined for example by using a Split Hopkinson Pressure Bar (SHPB) system. Bear in mind that the strength of the in situ rock mass is always less than the laboratory strength of an intact sample of the mass due to the discontinuities in the rock mass (Zhang 2016; USDA 2012).

2.3 Blast induced stress waves

During detonation, two types of stress waves are transmitted into the rock mass: longitudinal waves called primary (P) waves and torsional waves called secondary (S) waves . The S-waves largely decrease or disappear in the rock mass due to their inability to propagate through discontinuities. The velocity of an S-wave is also always much lower than that of a P-wave (Zaid 2016; Zhang 2016).

The P-wave velocity c_p (i.e. sonic velocity) of rock can be determined by:

$$c_p = \sqrt{\frac{E(1-v)}{\rho(1+v)(1-2v)}} \tag{3}$$

where ρ is the density, v is Poisson's ratio, and E is the Young's modulus of a rock (Zhang 2016). For rocks, the value of Poisson's ratio (the ratio of lateral strain to axial strain at linearly elastic region) is usually between 0 and 0.5; the range of 0.05 to 0.45 covers most rocks (Gercek 2007) and 0.25 is suitable for many rocks (Zhang

2016). Young's modulus measures the rock's ability to withstand deformation and can be defined with UCS tests. The higher the value, the harder the rock will be to break (Read J. & Stacey 2009; Małkowski et al. 2018).

The original stress wave caused by blasting is a compressive wave with a small tensile tail. A waveform has an almost vertical front (peak) that quickly decreases. The amplitude of the initial wave equals the explosive-produced gas pressure [Pa] (or the stress [Pa]) in the rock mass. The stress wave length is greatest at the initiation point and it mainly depends on the time during which the detonation gases completely escape out of the location. The borehole pressure duration is 8 to 13 times longer than the detonation time, so the stress waves in rock mass caused by blasting are much longer than corresponding detonation time (Zhang 2016; Read & Stacey 2009).

When a blast-induced compressive stress wave reaches a rock-air interface, such as an open joint or free surface on the bench face, the compressive stress wave is reflected back as a tensile wave (Figure 3). The reflection of the stress wave follows Snell's law (Zhang 2016). So, initially, the angle β of the reflected tensile wave from the free surface is equal to the angle α of the incident compressive stress wave. As the detonation of the emulsion column progresses, the angle changes. In the illustrative figures of this thesis, it is assumed that the VOD and the P-wave velocity of the rock mass are equal.

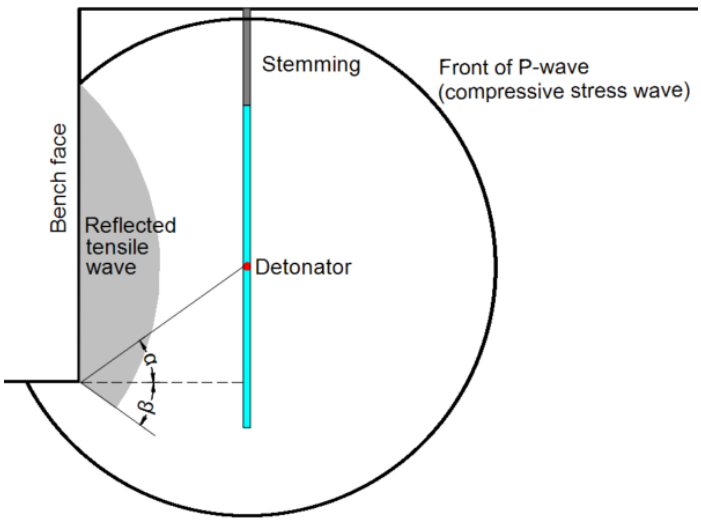

Figure 3. Stress waves in bench blasting.

2.4 Rock breakage mechanism

The currently accepted mechanism of rock blasting indicates that rock fragmentation results from gas flowing and stress waves. The energy source for both are the extremely high-pressure gases produced by the chemical reaction of the explosives (Zhang 2008). When the stress exceeds the strength of the rock at a given point, fracturing occurs in a manner that is defined by the physical properties of the rock mass (Parra Galvez 2013).

When an explosive is detonated, a shock wave is caused and the shock pressure usually exceeds the compressive strength of the rock by many times, as a result, the blasthole expands and a crushed zone is formed. This crushed zone formation can consume much energy released by blasting and it reduces the pressure to the point where the shock wave attenuates to an elastic (or elastoplastic) stress wave. Due to the rapid attenuation, the effect of shock wave on rock breakage decreases with increasing distance from the blasthole (Zhang 2008; Read & Stacey 2009; Chen et al. 2018).

The initial compressive stress wave from blasting compresses the rock radially, which results in tangential tension. If the tangential stress is greater than the tensile strength of the rock, radial cracks are induced in the radial directions, forming a fractured zone. The fractured zone extent is mainly determined by the radial cracks in the remained rock mass. In the near field of a blasthole shock waves, shear and tensile failure are the major contributors to rock fragmentation (Zhang 2016; Read & Stacey 2009; Chen et al. 2018).

The compressive stress wave continues to attenuate as it travels through the rock mass. When reaching a free surface the wave is reflected back as tensile stress wave. If the tensile wave amplitude exceeds the tensile strength of the rock, the tensile fracture called spalling will begin close to the free face. The greater the compressive wave, the greater the reflected tensile wave and thinner the spalling. Thus, fragmentation is better with smaller burdens. As the fracture caused by the tensile wave reaches the radial cracks, a net of cracks is created and the generated gases will begin to escape to the atmosphere. When all the gases are released into the air, the pressure acting on all fragments decreases to the atmospheric pressure. In open pit rock blasting, the rock between crushed zone and free surface is mainly destroyed due to tensile failure (Awuah-Offei 2018; Zhang 2016; Read & Stacey 2009). The breakage mechanism is shown in Figure 4.

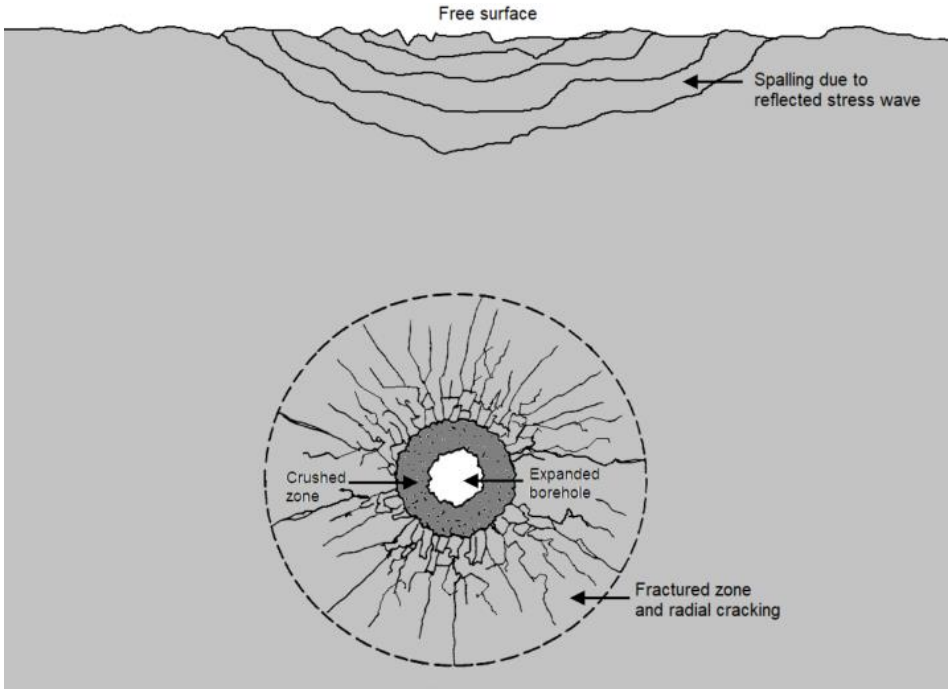

Figure 4. Rock breakage mechanism in blasting.

The blast-induced stress wave propagates much faster than the cracks. The maximum velocity of crack propagation in rocks or rocklike materials has measured to be 33% and the mean crack velocity 8 – 30% of the P-wave velocity (Zhang 2016). For example, assuming the crack velocities of 8 – 30% of the P-wave velocity and 5.4 m burden used in waste rock blasting in Kevitsa, then the reflected tensile stress wave reaches the radial cracks when the cracks have propagated 0.8 – 2.5 m from the blasthole.

The gas pressure in the borehole directly correlates with the degree of fragmentation. The performance of an explosive is often evaluated by its VOD. Higher VOD corresponds to a higher detonation pressure, resulting in greater stresses and higher energy concentration in the surrounding rock. Thus, rock fragmentation has a strong correlation with VOD. To achieve good fragmentation, VOD should be matched with rock properties and should be always equal to or greater that the P-wave velocity of the rock (Zhang 2016; Awuah-Offei 2018; Konya & Konya 2018).

Figure 5 illustrates a situation where the P-wave velocity c_p of the rock mass is twice the VOD, the detonation of the explosive column is initiated from the bottom, and half of the explosive column has already detonated. As we can see, the compressive wave has reached the explosive column before the detonation has ended and the backup detonator on top of the column is still unfired. This may lead to detonation failures and damage of detonators, and should be avoided (Zhang 2016).

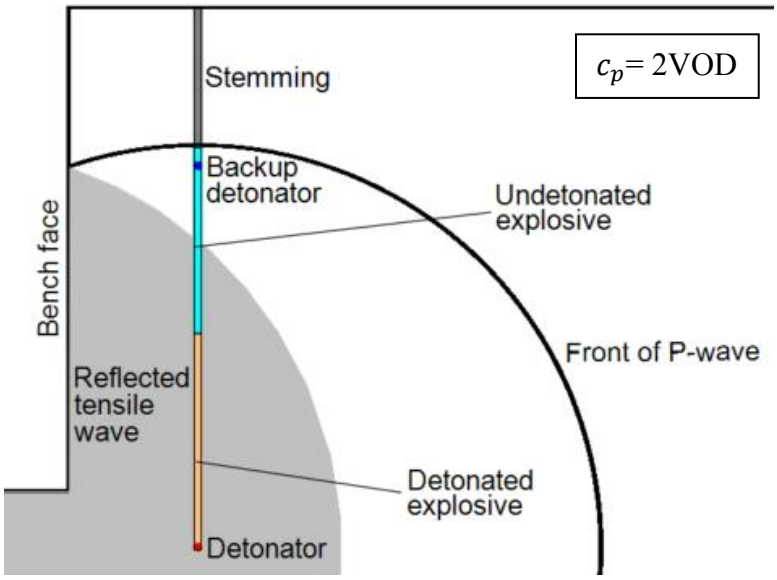

Figure 5. Possible explosive failure due to too low VOD.

For example, the measured VOD of the emulsion explosive currently used in Kevitsa is 5800 m/s in average and according to the Sonic Log drill hole measurements the average P-wave velocity of Kevitsa rock mass is 6868 m/s. Lower VOD may cause problems with blasting and worsen fragmentation.

2.5 Shock wave propagation through interfaces and role of stemming

In rock blasting, the propagation of shock wave occurs through the explosive-rock and explosive-stemming interfaces as shown in Figure 6. When a blast-induced shock wave (incident wave) reaches a stemming or rock, part of the wave is transmitted into the stemming or rock (transmitted wave), and the other part reflects back into the blasthole (reflected wave) (Zhang 2016).

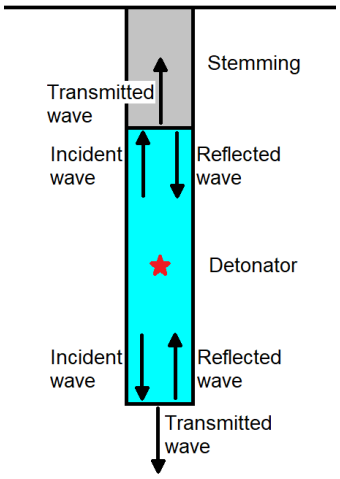

Figure 6. Shock wave propagation through interfaces.

Shock wave behavior at an interface depends on the characteristic impedance difference between the materials. The characteristic impedance of a medium can be mathematically represented by:

$$Z = \rho c_p \tag{4}$$

where ρ is the material density [kg/m^3]. If shock propagates from low to high impedance material, the shock pressure increases and vice versa. Thus, if the impedance of the explosive is smaller than the impedance of stemming or rock, the shock pressure increases and correspondingly, if the impedance of the explosive is greater, the pressure reduces. Therefore, the high impedance stemming material should be favorable to rock fragmentation (Zhang 2016).

For example, the characteristic impedance of the emulsion explosive currently used in Kevitsa is ~7.4x10^6 kg/m^{2}s (with VOD = 5800 m/s and ρ = 1.27 g/cm^3). In terms of fragmentation and energy efficiency, the impedance of stemming and rock should be greater than this. Unfortunately, the blasthole bottoms often consists of drilling fluids whose characteristic impedance has been studied by Mozie (2017), reporting an average impedance of ~2x10^6 kg/m^{2}s for water-based drilling fluids. Thus, drilling fluids (or water) at the blasthole bottom are problematic. A pure rock interface should not be a problem, since e.g. the computational characteristic impedance of the Kevitsa rock is ~15.8x10^6 kg/m^{2}s (with ρ = 3.17 g/cm^3 and c_p = 5000 m/s).

Stemming is one of the most important aspects of the blast design and the stemming material and size of the material greatly affect the blast result (Zhang 2016; Konya & Konya 2018). The most important functions of stemming is to keep the explosive energy within a blasthole and to reduce energy loss from the collar (Zhang 2016). Without stemming, the energy escape through the collar can be up to 50% of the explosive energy (Brinkmann 1990). A stemming material such as aggregate reduces the premature venting of high-pressure gases into the atmosphere. With use of proper stemming material and stemming length pressure losses can be minimized, energy efficiency increased, and fragmentation improved. Wetting of stemming material can greatly reduce the effectiveness of stemming (Konya & Konya 2018).

The optimal size of the stemming material is usually considered to be based upon the size of the blasthole. A proper sized stemming material can decrease the amount of stemming needed on a blast by over 30% (Konya & Walter 1990). According to Jimeno et al. (1995), the most effective stemming is achieved with particle sizes between 1/25 and 1/17 of the blasthole diameter. Investigations carried out by Otuonye (1981) indicate that the stemming length could be reduced by up to 41% by using the stemming material size $\emptyset_{st}$:

$$\emptyset_{st} = \frac{1}{25}\emptyset \tag{5}$$

where $\emptyset$ is the blasthole diameter. However, this is an empirical formula and further research is needed to determine an optimum stemming.

3 THEORETICAL STUDY

In this part of the thesis, Kevitsa's blast designs are studied and analyzed in theory. The theoretical study compares current blast design with optimal one, regarding the effect of detonator position on fragmentation.

3.1 Current blasting in Kevitsa

The Kevitsa open pit is mined in 12 m benches with 1.5 m subdrilling. Production holes are 165 or 225 mm in diameter and drilled in staggered pattern. The design parameters for waste rock and ore blasting for different hole sizes are presented in Table 1. Compared to ore blasting, the burden and spacing of waste rock blasting are wider, thus the powder factor is smaller; bench height, subdrill, stemming, and emulsion column length are equal.

Table 1. Basic blast design parameters for blasting in Kevitsa.

Hole size Ø	Waste 165 mm	Waste 225 mm	Ore 165 mm	Ore 225 mm
Bench height [m]	12	12	12	12
Subdrill [m]	1.5	1.5	1.5	1.5
Burden [m]	4.2	5.4	3.7	4.8
Spacing [m]	4.8	6.2	4.3	5.5
Stemming [m]	3.5	4.5	3.5	4.5
Emulsion column length [m]	10	9	10	9
Powder factor [kg/m^3]	1.1	1.1	1.4	1.4

As always, reality depends on the field conditions and the blasted bench height usually ranges from 12.5 to 13 m due to the remaining 0.5 – 1 m uneven layer of toes or otherwise hard, unloaded upper bench bottom. The main blasting problems at Kevitsa include:

- Thick loose rock layer at the top of the bench
- Floor humps / toes / poor bench floor diggability
- Damaged zone (blast damage) from the previous blast

The loose rock layer at the top of the bench is usually from one to three meters, but can be up to 6 meters. Loose rock often cause blastholes to collapse, resulting in that the blastholes cannot be charged, or that the fragments fall to the bottom of the blastholes causing the drilled depth to deviate from the actual charged hole depth, so that actual

emulsion column is shorter than designed. Thus, the loose rock layer is probably the main source for floor humps / toes and poor floor level diggability.

Non-electric Exel detonators cover 70% of the production blasts in Kevitsa, and electronic IKON detonators are used for the rest 30%. Two detonators are set to each blasthole. One is placed about 1 – 1.5 m above the hole bottom, to prevent the possible drilling fluid-emulsion mixture at the bottom. The other is placed somewhere between 3.5 – 8 m below the bench surface, depending on the stemming length (or hole size) and how the emulsion column is lifting the detonator. In practice, the usage of non-electric and electronic detonators corresponds to two different cases:

1. Single-detonator system: With non-electric detonators the primary detonator is placed 1.5 m above the hole bottom and the backup detonator on top is initiated with a delay of 25 ms if the bottom does not detonate.
2. Double-detonator system: With electronic detonators both (bottom and top) detonators are initiated at the same time.

3.2 Detonator position theory

Although very little known, a detonator position is one of the most important factors influencing rock fragmentation. Non-optimal placement at the bottom of the blasthole, or worse, on the top of the explosive column is very commonly used. Based on the stress wave theory, fragmentation improves by placing detonators in the middle of the explosive column (Zhang 2005; Zhang & Naattijärvi 2006; Zhang 2008; Zhang 2016). Studies by Zhang (2005), Brunton et al. (2010), and Menacer et al. (2015) have verified this theory.

In this thesis, the effect of detonator position is studied by changing the detonator placement near the theoretical optimum in both of the detonator systems used in Kevitsa. The double-detonator system has two advantages over single-detonator system: 1) The stress distribution is more even resulting in better fragmentation, and 2) shock wave collision happens resulting in higher pressure and stress in the surrounding rock mass, thus better fragmentation (Zhang 2016).

3.2.1 Stress distribution and energy efficiency

As mentioned before, rock fragmentation depends mainly on total energy used in fragmentation and stress distribution in the rock mass. In terms of energy efficiency, as much detonation energy as possible in each blasthole must go into the surrounding rock to be fragmented (Zhang 2016). In open pit blasting, the energy loss from the collar can be avoided by using proper stemming.

Single-detonator system

Figure 7 shows the compressive and tensile stress wave distribution in a single-detonator system at three different detonator positions A, B, and C at the moment when the detonation has propagated ½ charge length from the detonator. The region covered by the stress waves is where the rock fracture begins in each option.

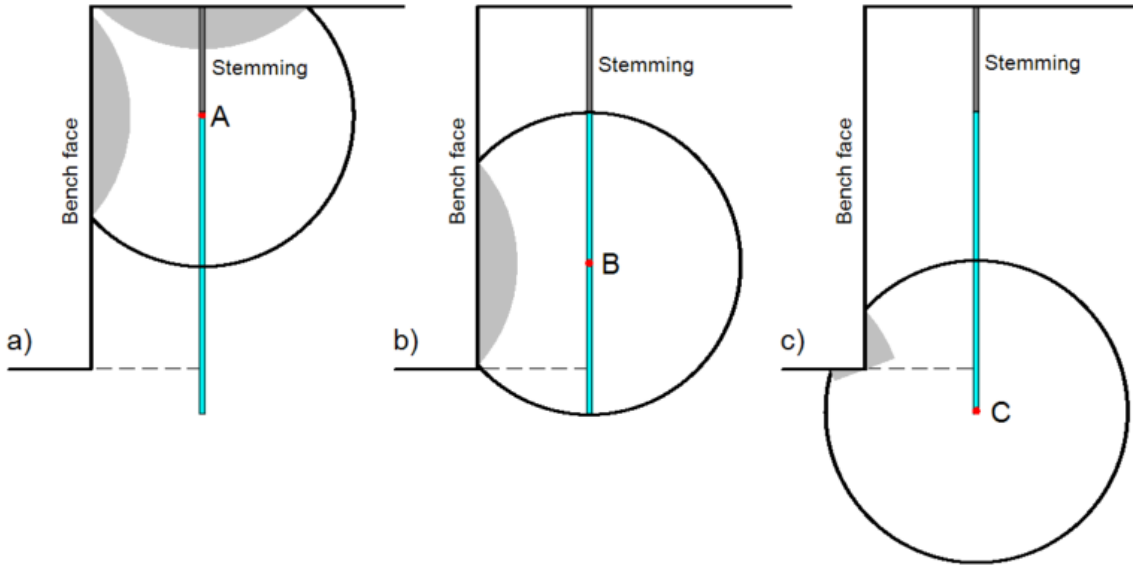

Figure 7. Stress wave distribution at the moment when detonation has propagated ½ charge length from the detonator with three different detonator positions: a) top, b) middle, and c) bottom of the explosive column. (Scale: Kevitsa ore blasting with 165mm hole size.)

The stress distribution and energy efficiency with different positions is as follows:

A) The stress is initially distributed at the top of the bench where the reflected tensile waves begin to tear the rock fragments towards the sky or open space in front of the bench. As we can see, the tensile waves can reach the blasthole before the

detonation has ended and some amount of explosive energy can escape through this broken region, leading to energy loss.

B) The stress is initially distributed to the bench that we aim to fragment and the burden begins to facture from the bench face. In this case, the entire explosive column is detonated before the tensile wave reaches the blasthole, thus there is little or no energy loss before the explosive detonation is completed.

C) The stress is initially distributed mainly below the bench and the tensile fracture begins from the bench floor level. The tensile waves can reach the blasthole before the detonation has ended and some amount of explosive energy can escape through this broken region, leading to energy loss.

Therefore, the best detonator position in terms of stress distribution, energy efficiency, and fragmentation is the middle position B.

The effect of detonator position on the distribution of stress waves between the middle position and Kevitsa's current practice in single-detonator system is shown in Figure 8. The scale of the figures corresponds to the waste rock blasting with a 165 mm hole size, and the stress distribution corresponds the situation when the detonation of the entire explosive column has ended. The red dot presents the primary detonator and the blue dot is the backup detonator.

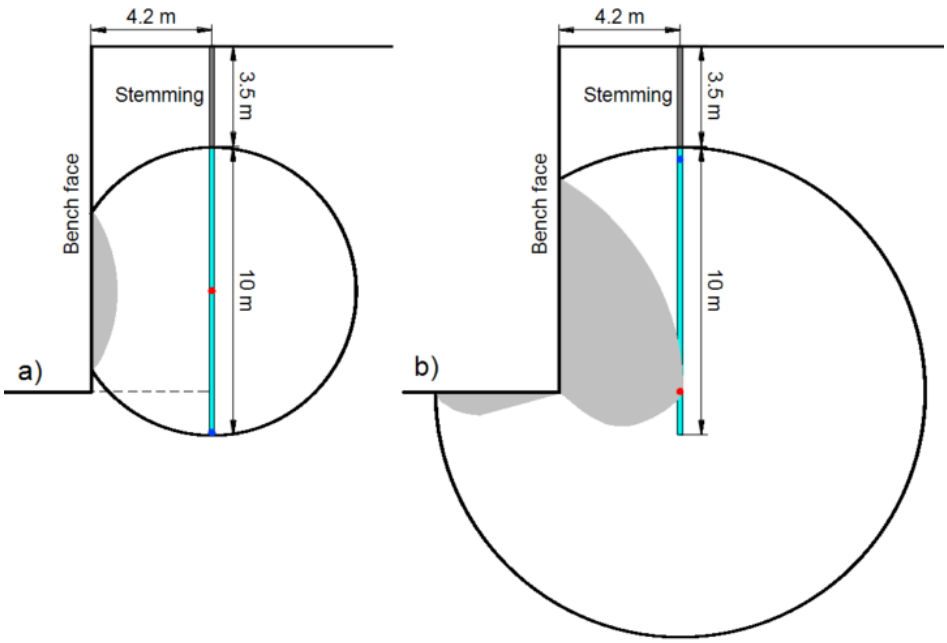

Figure 8. Stress wave distributions at the moment when detonation of the explosive column has ended: a) middle position, b) current position. (Scale: Kevitsa waste rock blasting with 165mm hole size.)

As we can see, in Figure 8a, representing the middle detonator position, the whole process of detonation lasts much shorter period of time and it happens within the rock to be blasted, meaning that detonation energy will mostly go into the bench to be fragmented, without energy loss during detonation. In Figure 8b, representing the current waste rock blast design in Kevitsa, the reflected tensile wave reaches the blasthole shortly before the entire emulsion column has detonated. In this case, a small amount of energy loss can occur when the reflected tensile fracture reaches radial cracks and gas begins to escape through that region. In ore blasting, the burden is 0.5 – 0.9 m smaller, so more explosive energy can be wasted. In current practice, the energy of the emulsion charge is distributed over a larger volume, meaning that the stress amplitude (i.e. peak pressure) is less, and fragmentation is worse.

One reason for the thick loose rock layer in Kevitsa could be that, with current practice, the stress distribution and rock fracture are more targeted to the bench floor. Theoretically, the loose rock layer could be reduced by placing the detonator upper in the emulsion column. Consequently, toe / floor hump / poor bench floor diggability problems could reduce as well when there are less loose rock fragments that can fall to the bottom of the blasthole and shorten the desired hole depth, or cause collapsed holes. Thus, the detonator position in the middle of the explosive column would be more favorable not just for fragmentation but also to reduce problems.

Double-detonator system

In a double-detonator system, stresses are distributed more evenly resulting in better fragmentation (Zhang 2016). Stress distribution with a few detonator position options is shown in Figure 9. The stress distribution equals the area, when detonation has advanced L/4 from the detonator, where L presents the length of the explosive column. As we can see, the best stress distribution is achieved when the detonators are placed at the positions of L/4 and 3L/4 in the explosive column. In Kevitsa, the stress distribution with current design varies a lot depending how the emulsion pumping has lifted the upper detonator, and the lower detonator 1.5 m above the bottom is placed lower than optimum (Figure 9a and 9b). In a double-detonator case, the entire explosive column is likely detonated before the tensile waves reach the blasthole, thus there is little or no energy loss before the explosive detonation is completed.

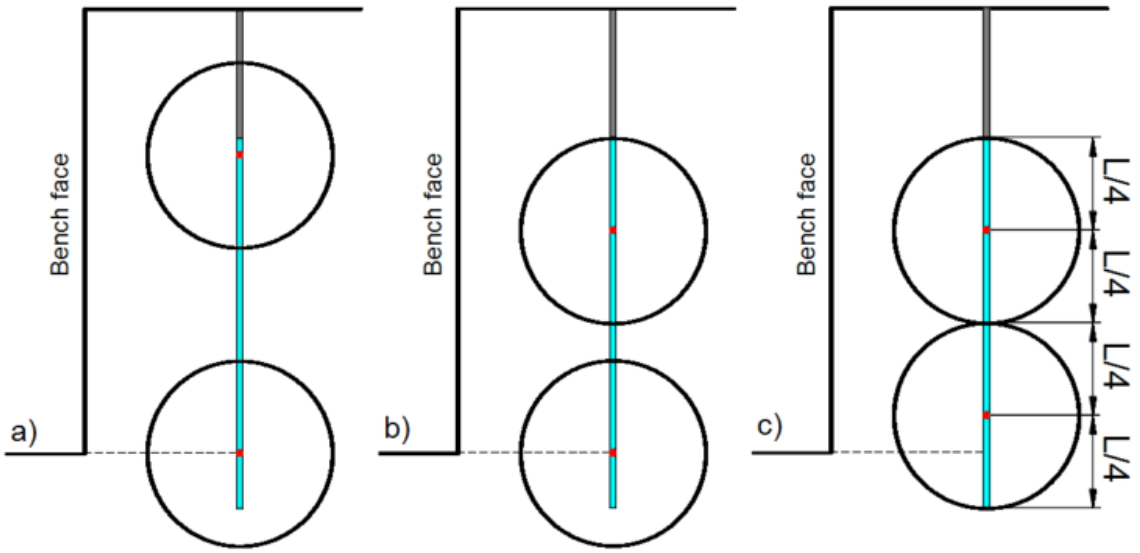

Figure 9. Stress distribution at the moment when the detonation has advanced L/4 from the detonator, with different detonator positions a), b) and c) in a double-detonator system. (Scale: Kevitsa waste rock blasting with 165mm hole size.)

3.2.2 Detonation time

The detonation time T_D depends on the explosive VOD, detonator placement and the charge length, as follows:

$$T_D = \frac{L_{max}}{VOD} \tag{6}$$

where L_{max} can be: (1) the maximum distance from a detonator to the end of the explosive column, or (2) in case of a double-detonator system it can be the distance between the detonators divided by two if the result is more than (1).

Shorter detonation time means that the total energy of the explosive is released to the rock mass faster as shown in Figure 10. The wave on the left damages the rock, but the wave on the right does not. A higher energy concentration and more even stress distribution should be better for rock fragmentation (Zhang 2016). In a single-detonator system, the detonation time can be halved by moving a detonator from bottom or top to the middle of the explosive column. In a double-detonator system, the detonation time can be further halved by placing the detonators at the optimum positions, as presented in Figure 9c.

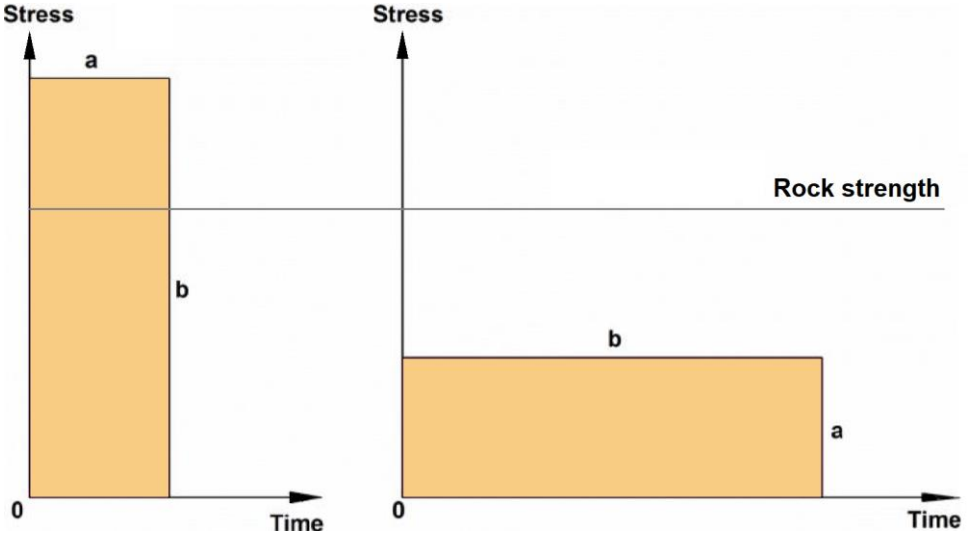

Figure 10. Two stress waves containing equal energy.

3.2.3 Loading rate

The sizes of fragments decrease with increasing loading rate (Zhang 2016). Loading rate ($d\sigma/dT_D$) may increase if the detonation time T_D is reduced. Thus, by placing the detonator(s) in optimum positions, the loading rate may be increased. The kinetic energy of flying fragments also increases with an increasing loading rate (Zhang et al. 2000; Zhang 2016).

3.2.4 Kinetic energy of the flying fragments

Energy released by the explosive is converted into different forms of energy. Measurements indicate that the percentage of measurable form of energy from the total explosive energy is the following:

Fragmentation energy 0.1 – 6.0%
Seismic energy 0.6 – 12%
Kinetic energy 3.3 – 39%

The maximum sum of these energies is 40% (Sanchidrián et al. 2007). According to dynamic tests, the kinetic energy can be up to 28% of the total input energy if burden velocity is 20 m/s. Therefore, kinetic energy carried by flying fragments in rock fracture is notable and this kinetic energy can be well used in secondary fragmentation and thus improve energy efficiency in blasting (Zhang 2017).

If the detonators are optimally positioned, the burden begins to facture from the bench face. When fragments are thrown towards the previously blasted fragments the kinetic energy carried by flying fragments can be used for a secondary fragmentation. With improper detonator placement, this advantage is partly lost.

In open pit mines, most boulders come from the first row. One of the main reasons is that the fragments can freely fly away, making the kinetic energy mostly wasted (Zhang 2019). For the following rows, too large space is neither cost-effective nor productive, and too small is not large enough to let fragments move away. Swelling ratio should be properly determined to further improve fragmentation (Zhang 2016).

3.2.5 Stemming length

As mentioned earlier, the most important functions of stemming is to keep the explosive energy within a blasthole and to reduce energy loss from the collar. In order to avoid or reduce the energy loss, the length of stemming should be correct (Zhang 2016).

In stemming, shock wave from detonated explosive will rapidly decay to a stress wave. When the wave travels to a collar, the reflected tensile wave begins to eject the stemming. After a certain time the entire stemming will be ejected. If we assume that the wave propagation in the stemming is a stress wave problem, and as soon as the detonation in the borehole is finished, all the explosive energy will be released, then the optimal stemming length can be determined based on stress wave theory. Thus, if the traveling time of the wave in the stemming to the free surface and back to the explosive-stemming interface is greater than the detonation time and the wave length measured at the explosive-stemming interface, there should be not energy loss from the collar (Zhang 2016).

The length of the detonation wave depends on the detonation time T_D and can be presented as mT_D, where m is a constant to be determined by experiments. The time during which the wave front is traveling from the explosive-stemming interface to the collar T_{st} can be presented as:

$$T_{st} = \frac{L_{st}}{c_{st}} \tag{7}$$

where L_{st} is the length of the stemming and c_{st} is the P-wave velocity of the stemming material (Zhang 2016).

In a single-detonator system, when detonator is placed in the middle or lower in the explosive column, the detonation wave reaches the stemming-explosive interface when the entire column is already fired. Thus, in order to avoid detonation energy wastage from the collar, the wave travel time in the stemming T_{st} and length of the detonation wave mT_D should correspond to:

$$2T_{st} \geq mT_D \tag{8}$$

As the wave travels twice the length of the stemming. Now the length of the stemming can be obtained from Equations 7 and 8 as follows:

$$L_{st} \geq \frac{1}{2} mT_D c_{st} \tag{9}$$

As we can see, the optimal stemming length is directly proportional to the detonation time T_D and if we substitute the T_D using Equation 6, we get:

$$L_{st} \geq \frac{L_{max}}{2} \frac{mc_{st}}{VOD} \tag{10}$$

In the current single-detonator system used in Kevitsa, the primary detonator is about 1.5 m above the blasthole bottom and explosive column lengths are 10 or 9 m for 165 and 225 mm holes, respectively. Thus, the maximum distance from a detonator to the end of an explosive column L_{max} is accordingly 8.5 or 7.5 m, and the corresponding stemming lengths using Equation 10 are:

$$L_{st\_D165} \geq 4.25 \frac{mc_{st}}{VOD} \tag{11}$$

$$L_{st\_D225} \geq 3.75 \frac{mc_{st}}{VOD} \tag{12}$$

By placing the detonator in the middle of the explosive column, the corresponding L_{max} would be 5 or 4.5 m and the corresponding stemming lengths:

$$L_{st\_D165\_middle} \geq 2.50 \frac{mc_{st}}{VOD} \tag{13}$$

$$L_{st\_D225\_middle} \geq 2.25 \frac{mc_{st}}{VOD} \quad (14)$$

Thus, theoretically, the current stemming lengths (3.5 and 4.5 m) could be reduced approximately 40% by placing the detonator in the middle and still keep the same amount of energy in the blasthole. Correspondingly, a similar analysis could be made for the double-detonator system.

Collar zone or stemming region of the blast is often the primary source of oversize boulders. The oversize on top of the muckpile can be reduced by reducing stemming length without jeopardizing adequate confinement (Singh & Narendrula 2010). The stress distribution in the bench is better with a sorter stemming. An optimal stemming length for Kevista should be studied and determined by experiments.

As described in Chapter 2.5, the optimal stemming length is also based on the stemming material, and the optimum size of the material is usually considered to based on the diameter of the borehole. According to the empirical formula shown in Equation 5, the size of the stemming material in Kevitsa should preferably be about 7 or 9 mm for the 165 or 225 mm holes, respectively. The stemming material currently used is screened to a size of 10 – 25 mm. A proper stemming material size for Kevitsa should be studied.

3.2.6 Rock confinement

Rock confinement is greatest at the bottom of a blasthole (Zhang 2016). Thus, by placing a detonator at the bottom, more energy is distributed to the rock mass in the form of seismic energy and is not used for rock fragmentation. By placing the detonator in the middle of an explosive column, there less confinement and more free surface to be favorable to tensile fracture. The current detonator position, 1 – 1.5 m above the bottom, in Kevitsa is not optimal in this sense either.

3.2.1 Stress wave superposition

Stress wave superposition is achieved when two separate stress waves overlap each other. If both of the waves have the same sign (i.e. both are compressive or both are tensile), they are directly superimposed, resulting in greater stress. By placing a detonator in the middle of an explosive column, the upward and downward propagating detonations both create separate stress waves. When these two detonation fronts overlap further from the

blasthole, a peak value of the stress amplitude increases. The amplitude of stresses in the rock mass surrounding a blasthole greatly affects rock fracture and fragmentation. Figure 11a shows a single stress wave induced by a detonator at the bottom of the blasthole, and Figure 11b shows the stress wave superposition when detonator is placed in the middle of the explosive column (Zhang 2016).

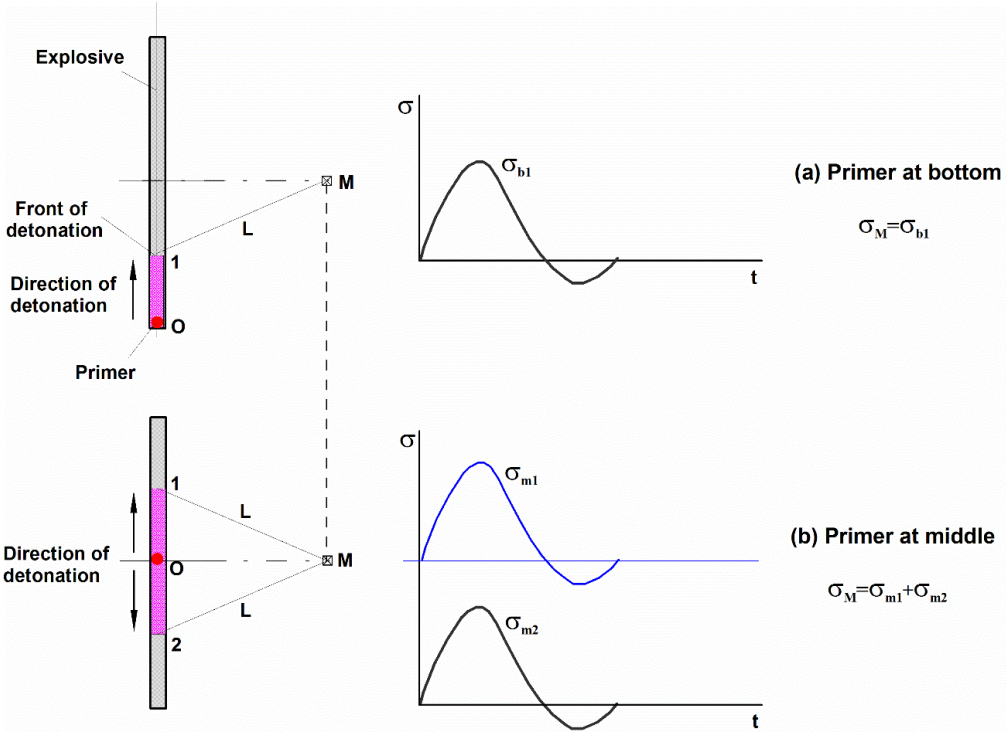

Figure 11. a) Stress wave induced by a detonator at the bottom of the blasthole. b) Stress wave superposition induced by a detonator in the middle of the explosive column (Zhang 2016).

3.2.2 Shock wave collision

The double-detonator placement is based on the principle of shock wave collision theory (Zhang 2016). In shock wave collision, the final shock pressure is greater than the sum of the original two shocks (Cooper 1996). If two detonators, placed at different positions in a single hole, are initiated at the same time, a shock wave collision occur between the detonators and the pressure increases. Accordingly, the final stresses produced by the shock collision are greater than the sum of the initial two stresses. This collision-caused high stress is beneficial to rock fracture and fragmentation (Zhang 2014; Zhang 2016).

The distribution of the stress waves with the optimal detonator placement is shown in Figure 12. When the detonation front from upper detonator propagates down and overlaps

with the detonation front from the lower detonator, the (orange) stress superposition region starts to form, resulting in greater stresses in the rock mass. With increasing time, this area expands outward (Zhang 2014).

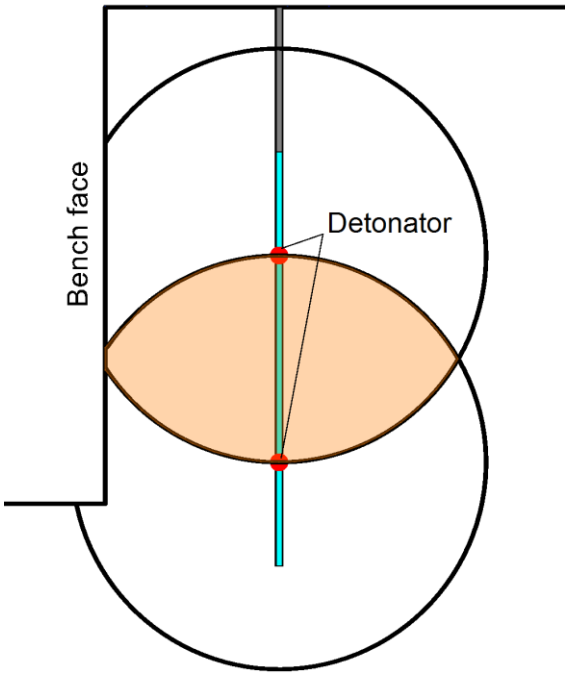

Figure 12. Stress distribution after shock wave collision in a blasthole.

4 CHARACTERISTICS OF KEVITSA ROCK

The mafic-ultramafic magmatism at ca. 2.06 Ga produced significant Ni-Cu-PGE resources in the Central Lapland greenstone belt, including Kevitsa layered intrusion (Makkonen et al. 2017). The deposit consists of very high to extremely high strength rock. Previous tests have shown an average UCS of 212 ± 71 MPa.

A higher amphibole content in the Kevitsa rock is expected to result in a worse fragmentation i.e. larger fragment size in the blasting. A clear correlation between the two has been observed in the enrichment process, especially in grinding. Thus, powder factor q in ore blasting has been adjusted according to the amphibolite concentration to achieve the desired fragment size for concentrating process. Powder factors for different blast designs are:

Waste rock	$q \approx 1.11$ kg/m^3
Ore – Normal Amphibole (< 45%)	$q \approx 1.41$ kg/m^3
Ore – High Amphibole (> 45%)	$q \approx 1.57$ kg/m^3

A higher powder factor is expected to result in finer fragmentation as more energy is applied to the same volume of rock.

In this thesis, Split-Hopkinson Pressure Bar (SHPB) tests were conducted to determine the correlation of the dynamic rock strength and amphibole content, and old fragment size data from machine vision cameras installed in shovels was analyzed to determine the correlation of the fragment size and amphibole content and in blasting.

4.1 SHBP tests – Rock strength in Kevitsa

Split Hopkinson Pressure Bar (SHPB) tests were performed on 15 rock samples to determine UCS of the Kevitsa rock under dynamic load. The tests were performed at the University of Oulu in November 2019. Amphibole content is based on XRD analysis of the samples. The test results are shown in Table 2. As mentioned in Chapter 2.2.1, the compressive strength of a rock increases with the increasing loading rate i.e. strain rate.

Table 2. The laboratory-measured dynamic UCS of Kevitsa rock.

Sample ID	Rock type	Amphibole content (%)	UCS (MPa)	Srain rate (s^{-1})	Shots
OMS-19-1	Olivine websterite / ore	19.54	184	62	1
OMS-19-2	Olivine websterite / waste	3.31	197	55	1
OMS-19-3	Olivine websterite / waste	84.16	204	71	2
OMS-19-4	Dunite / waste	36.60	228	59	2
OMS-19-5	Olivine websterite / false ore	17.91	211	55	3
OMS-19-6	Olivine websterite / waste	20.75	218	37	1
OMS-19-7	Olivine websterite / ore	15.11	218	30	1
OMS-19-8	Dunite / ore	15.69	191	20	1
OMS-19-9	Olivine websterite / ore	28.10	211	11	3
OMS-19-10	Olivine websterite / ore	18.95	191	15	4
OMS-19-11	Olivine websterite / waste	79.69	238	28	1
OMS-19-12	Olivine websterite / waste	80.97	231	51	1
OMS-19-13	Olivine websterite / ore (low grade)	69.77	259	29	4
OMS-19-14	Olivine websterite / ore	1.89	252	20	3
OMS-19-15	Olivine websterite / ore	17.07	245	34	1

The strength of some samples was too high so that they were not broken during the first shot. Each shot produces micro cracks and weakens the rock. Thus, multiple shots on the same sample results in a lower UCS value than actual rock strength. In addition, the samples OMS-19-6 and OMS-19-15 were not broken sufficiently enough, so the measured UCS is also lower than actual. Samples with UCS values greater than those measured are highlighted with grey in the table. Figure 13 shows examples of shot samples.

a)

b)

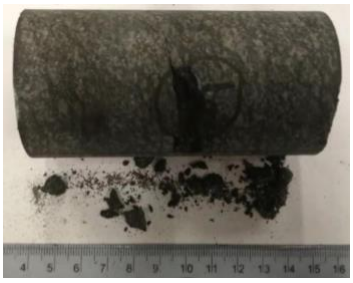

c) 

Figure 13. Rock samples a) Sufficiently broken OMS-19-2 and OMS-19-11, b) not-sufficiently broken OMS-19-6 and OMS-19-15, c) broken at the weakness zone OMS-19-3 and OMS-19-7.

The UCS values vary from 184 to 259 MPa. The samples with the greatest strength (OMS-19-13 and OMS-19-14) were shot three to four times before the sufficient fracture, suggesting that the maximum UCS of the Kevitsa rock is much more than 259 MPa.

Figure 14 shows rock UCS values compared to amphibole content of each sample. Grey markers on UCS line mean that the true UCS value is higher than the curve indicates. As we can see, there is no correlation between rock dynamic UCS and amphibole content.

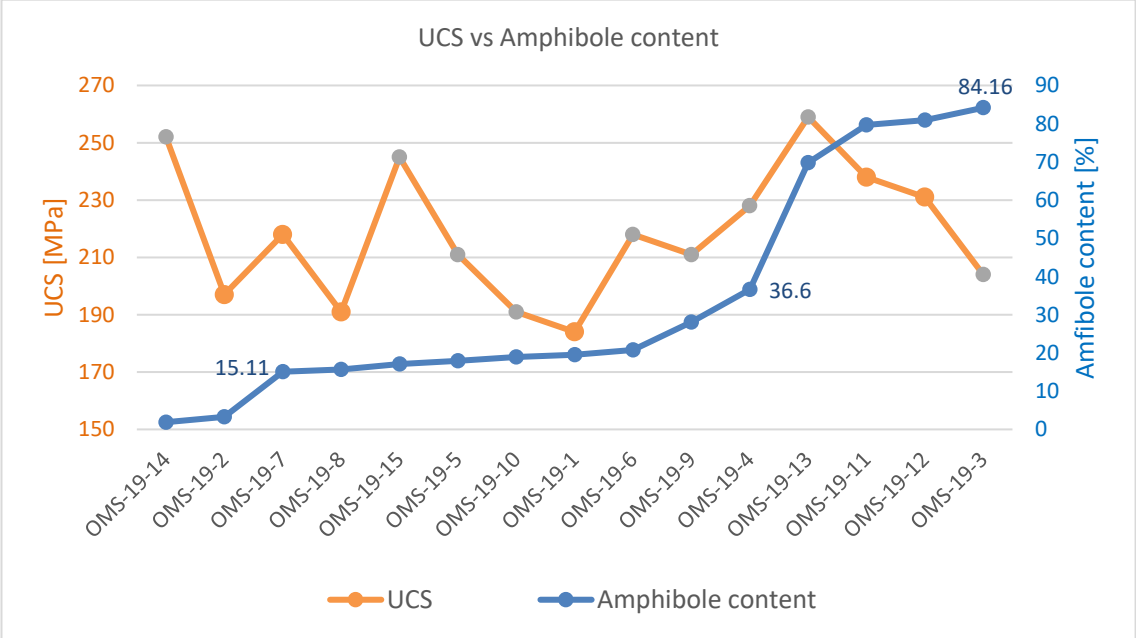

Figure 14. Rock UCS vs amphibole content. Gray values are actually greater than in the graph.

4.2 Effect of rock amphibole content on fragmentation

Effect of amphibole content on fragmentation was analyzed based on old fragment size data gathered with shovel-mounted machine vision cameras. The purpose of the analysis was to determine the correlation of amphibole content and fragment size in blasting. The data set consisted of 87 loaded ore blocks and 168 waste rock blocks. One loading block consists of many10x10x12m block model blocks and the amphibole content within one loading block can vary a lot. The average amphibole content of each loading block was calculated using the block model.

The blocks above level 1150 (weathered rock) were removed from the analysis. After that, the blocks were classified into different classes according to explosive and detonator, blasthole diameter, and blast pattern size. So that the parameters and powder factor in one class were constant. The classes with the maximum number of blocks having the same parameters were selected for analysis. Thus, 19 ore and 17 waste rock blocks listed in Appendices 1 and 2, were used in the analysis. The classes with maximum number of blocks are shown in Table 3.

Table 3. Analyzed classes for ore and waste rock blocks.

Class	Ore	Waste rock
Explosive	Fortis Extra	Fortis Advantage
Detonator	NONEL	NONEL
Blasthole diameter	225 mm	165 mm
Blast pattern size	4.4 x 5.2 m	3.8 x 4.4 m
Number of blocks	19	17

The blocks were divided into groups based on their amphibole content and an average percent of passing of 20, 50, and 80% (K20, K50 and K80) were counted for each group. Results are shown in Figure 15. As we can see, the trendlines for average fragment size (K50) are almost constant regardless of the amphibole content of the rock. Thus, based on this analysis there is no correlation between fragment size and amphibole content of rock in blasting.

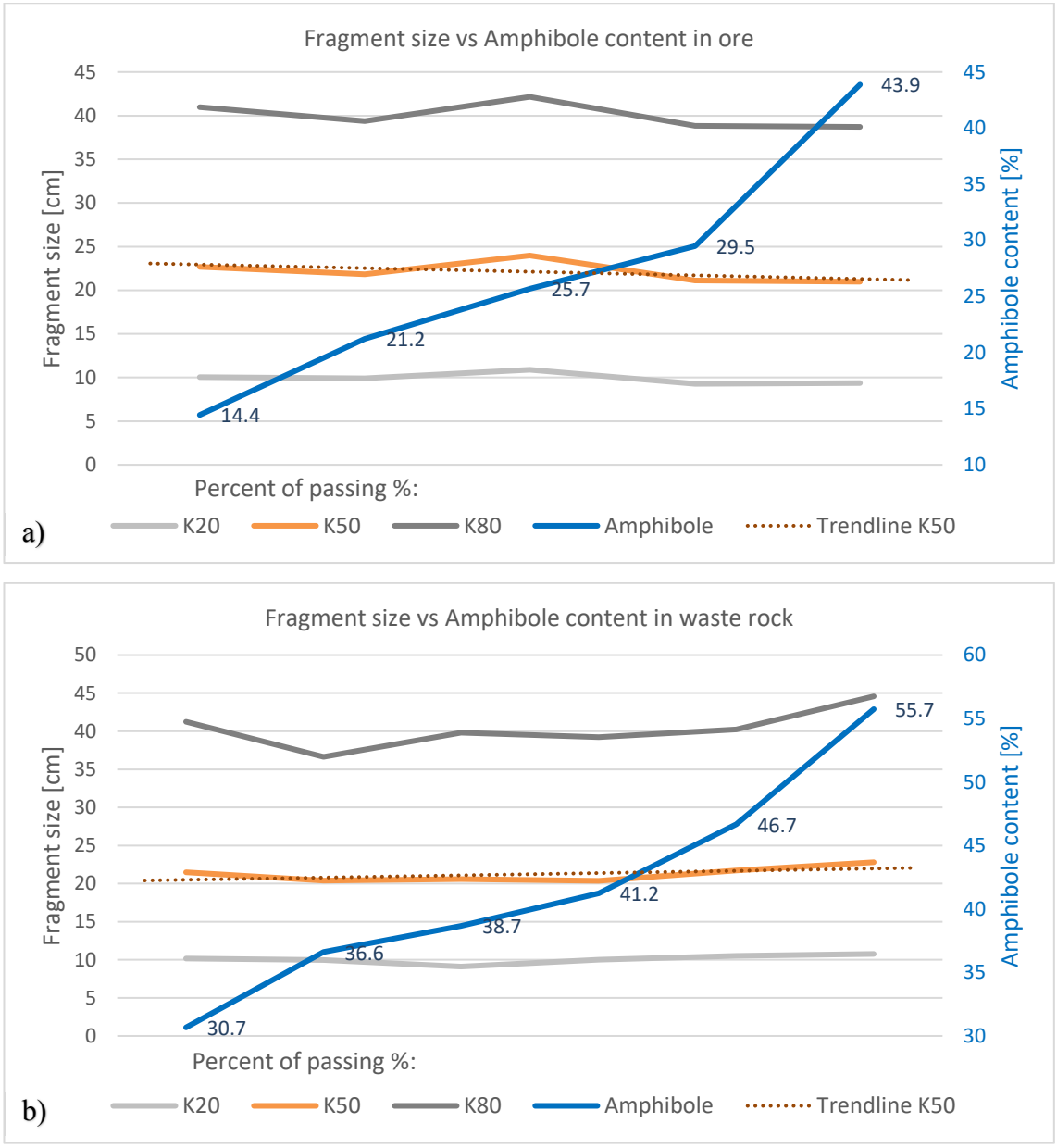

Figure 15. Fragment size vs amphibole content in a) ore blasts and b) waste rock blasts.

5 FIELD BLASTING TESTS

The purpose of the field tests was to determine the effect of detonator position on fragmentation in practice. The practical investigation was carried out in three different test fields. Kevitsa's current blasting practice was compared to a test design that represented a theoretical optimum in which detonators were placed at middle of the explosive column. To minimize the effect of rock and rock mass properties, part of the test field was charged according to the test design and the other part with the current practice, and the results were compared between these two areas. The basic design parameters for the test fields are presented in Table 4. All test fields were charged with a single-detonator system.

Table 4. Summary of test field parameters.

Blast field	C1078R013	C1078R011	C1066M003
Rock type	waste rock	waste rock	ore
Hole size Ø	165 mm	165 mm	165 mm
Hole depth	13.5 m	12 m	13.5 m
Burden	4.2 m	4.2 m	4.2 m
Spacing	4.8 m	4.8 m	4.8 m
Stemming	3.5 m	3.5 m	3.5 m
Emulsion column height	10 m	8.5 m	10 m
Designed Powder factor	1.340 kg/m^3	?	1.156 kg/m^3
Actual Powder factor	1.393 kg/m^3	?	1.217 kg/m^3
Muckpile movement direction	SE	W	NW

The test field C1066M003 was ore field but drilled with waste rock blast pattern size. The difference in the powder factors between the fields C1078R013 and C1066M003 is explained with extra blast holes drilled to the near bench face region, and the actual bench surface level that can deviate from the target level, thus effecting on the blasted tonnages. The test field C1078R011 was blasted together with other field, the powder factors reported by explosive company included both fields and could not be separated. The designed powder factor is always smaller than actual because the extra holes near the bench face are not included to the designed powder factor.

5.1 Test field C1078R013

Test field C1078R013 is shown in Figure 16. The test field was a small waste rock blast field and the test area and the conventionally charged reference area were loaded partially mixed. The blue highlight shows the reference area, counted as “current practice” in the fragment size data. The orange highlight was in the test area. As we can see, some amount of fragments have been mixed in the results between the reference and the test area. The area between the polylines was leaved out of the study because loading was performed on both sides of the field and could not be separated in the results. There were five collapsed holes (red dots) in the field in total and one fracture zone was piercing the field.

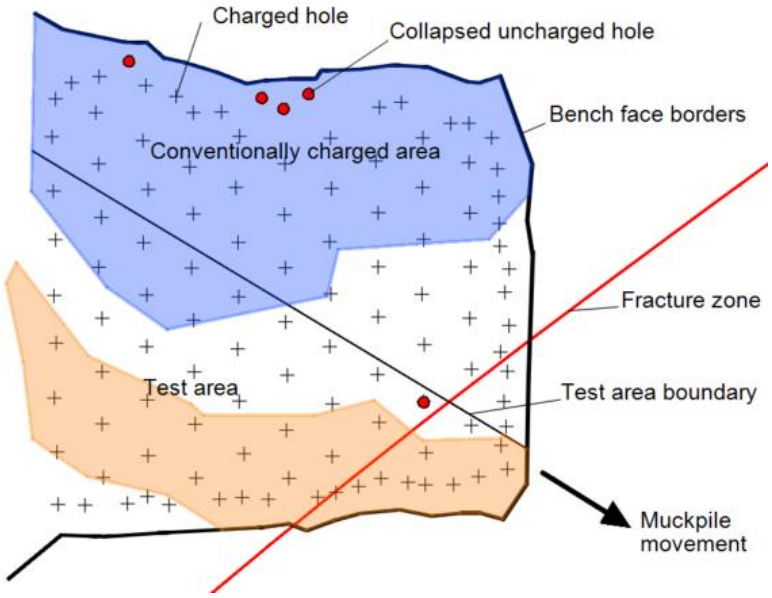

Figure 16. Test field C1078R013 data blocks and factors influencing data.The field above the test field was not loaded to the targed elevation. The loose rock layer above the target elevation was 0.75 - 1.5 m (Figure 17).

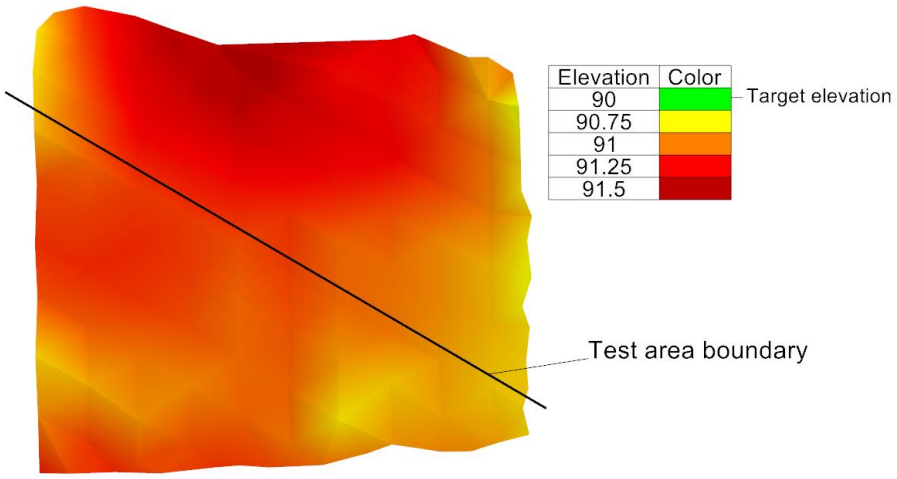

Figure 17. Elevation of the bench surface.

The reference area was charged according to the current practice (Figure 18a). In the test area, a primary detonator was lifted 4.5 - 5 m above the hole bottom, and a backup detonator was placed at the hole bottom (Figure 18b). The detonators in the test area were mounted by taping the primary detonator on backup detonator signal tube and gripping the backup detonator to the bottom of the borehole during emulsion pumping (Figure 18c).

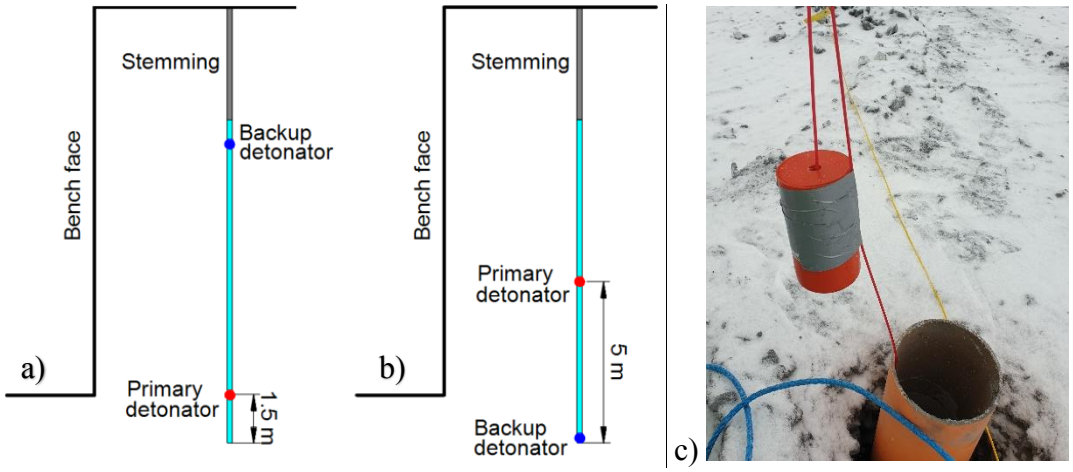

Figure 18. Detonator positioning in a) conventionally charged and b) test area in test field C1078R013, and c) primary detonator taped on backup detonator signal tube.

The test field C1078R013 was a small test field that served as road base and working area after the blast, thus test drillings to determine the loose rock layer below the blasted field could not be performed.

5.2 Test field C1078R011

Test field C1078R011 is shown Figure 19. The field was a waste rock blast field next to the permanent pit wall and on top of the catch bench. Subdrilling was not used and the depth of the blastholes were 12 m. The field was divided into loading blocks, from which UNW28, UNW29, UNW30, and USW11 were counted in the data analysis. The blue highlight shows the conventionally charged reference area, counted as “current practice” in the fragment size data. The orange highlight was in the test area.

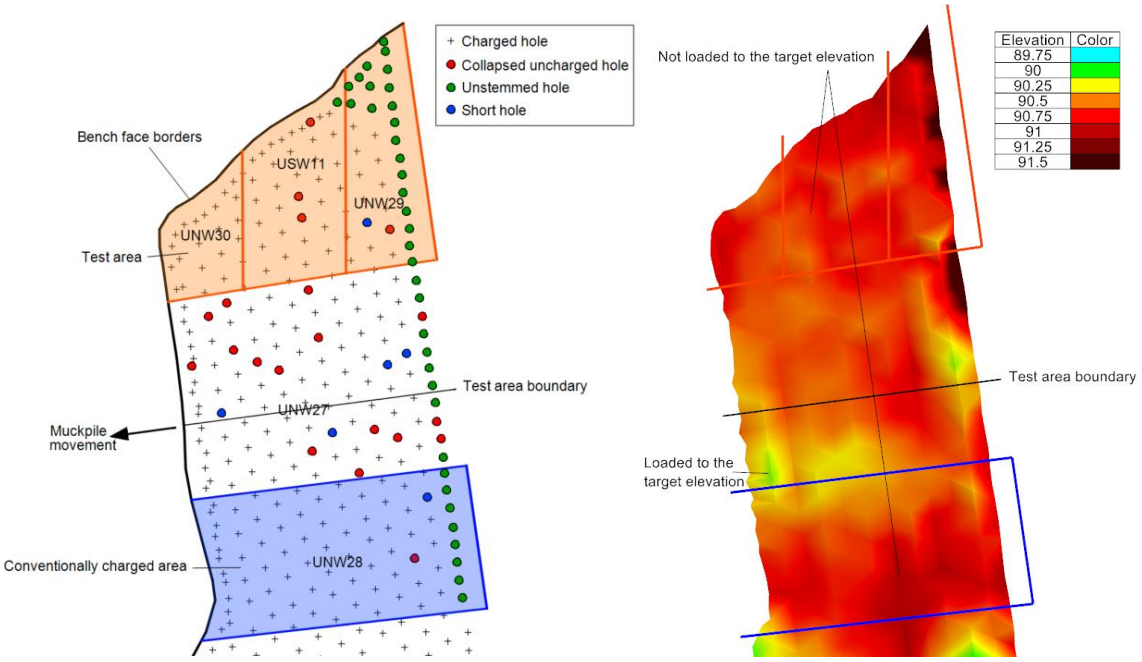

Figure 19. a) Test field C1078R11 data blocks and factors influencing data. b) Elevation of the bench surface.

The field was far from optimal; most of the holes were wet and the area between the study areas was leaved out of the study because of too many collapsed holes (red dots). There were 20 collapsed holes in the field in total. In addition, one corner of the test area was left unstemmed (green dots). In practice, all buffer holes next to the presplit holes are left unstemmed. In addition, the field above the test field was not loaded to the targed elevation (Figure 19b) and the loose rock layer above the target elevation in the study areas was more than 0.75 m, in average.

In this field, there was a small change to the current practice; both detonators (primary and backup) in one blasthole were installed 1-1.5 m above the bottom and initiated at the same time (Figure 20a). In the test area, detonators were lifted about 4 m above the hole bottom during the emulsion pumping by pulling the signal tube, to get them approximately in the middle of the explosive column (Figure 20b). Installing into the exact location was difficult and sometimes the detonators started to rose with the emulsion statue and had to be reinstalled into the emulsion by quickly lifting the bulk emulsion loading hose. This can lead to water-emulsion mixture that will impair the emulsion properties and end result.

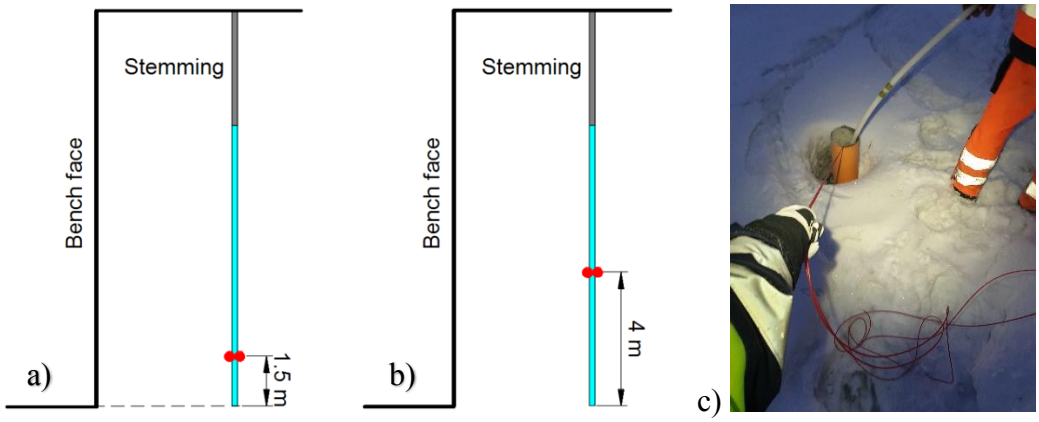

Figure 20. Detonator positioning in a) conventionally charged and b) test area in test field C1078R011, and c) detonator installation by pulling the detonator signal tube.

The test field C1078R011 was on top of the catch bench and the test area was in front of a ramp, thus test drillings to determine the loose rock layer below the blasted field could not be performed.

5.3 Test field C1066M003

Test field C1066M003 is shown in Figure 21. The field was an ore blast field. The field was divided into loading blocks, from which HG73, HG74, HG75, HG76, and HG77 were counted in the data analysis. The blue polyline shows the conventionally charged reference area of the field that was counted as “current practice” in the fragment size data. The orange polyline was the test area. The area between the polylines was left out of the study because of too determinant geological factors (three fracture zones were piercing the field) and too many collapsed holes (red dots). The locations of the fracture zones at the middle bench level are shown in Figure 21a. In addition, the field above the test field was not loaded evenly. According to a drill automation data there was a loose rock layer on top of the test area, and not a toe (Figure 21b). The detonators were mounted in the same manner as in the test field C1078T013 (Figure 18).

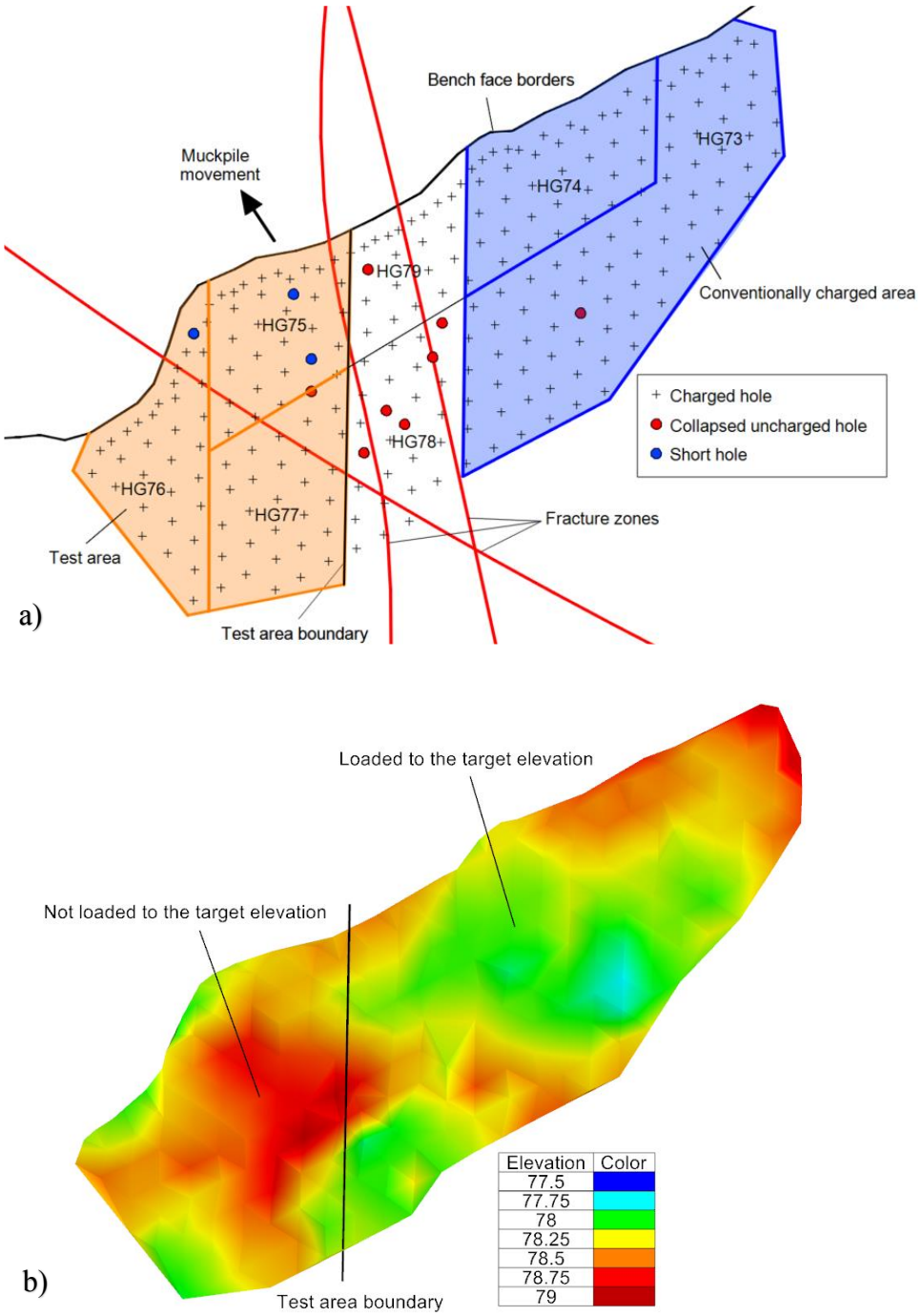

Figure 21. a) Test field C1066M0003 and factors influencing data. b) Elevation of the bench surface.

The test drillings were performed after loading of the test field to determine the loose rock layer below the blasted field. A total of 16 test drillings were designed to the field, but in practice only four holes were drilled in the test area and six in the reference area, as shown in Figure 22. The problematic areas, such as fracture zones and collapsed holes, were avoided.

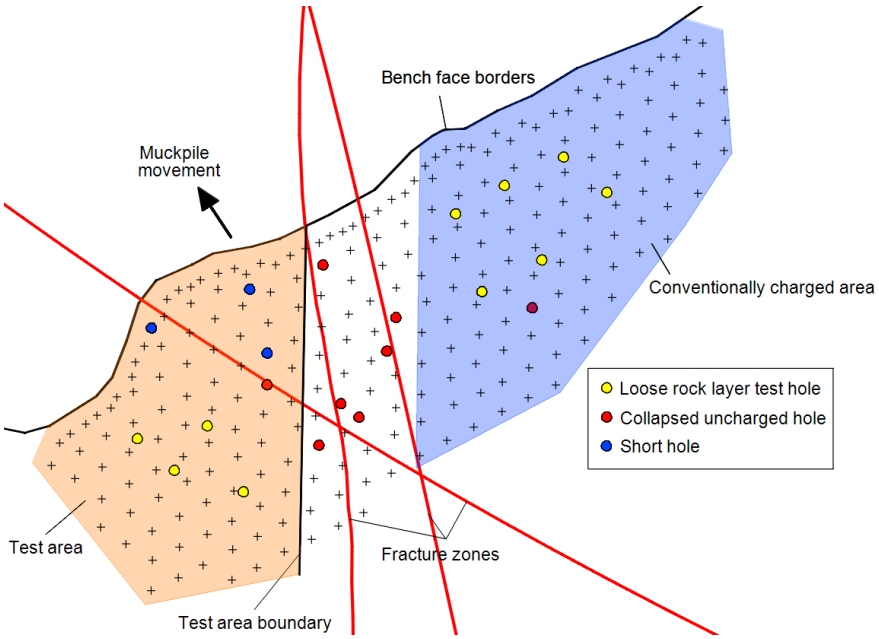

Figure 22. Loose rock layer test holes, the fracture zones on the bench floor level, and blasting problems on the test field C1066M003.

6 FIELD TEST RESULTS

The results were collected using three different methods:

1. The fragment size distribution, fragment sizes (K20, K50 and K80), and percentage of small size (< 0.025 m) and large size fragments (> 1 m) were measured using machine vision camera technology installed in the shovels. The cameras take pictures of a muckpile every three minutes, in average.
2. Loading machine operator feedback forms were collected from each field.
3. Test drillings were made to determine the loose rock layer below the blasted field where possible.

In addition, a slow motion video camera was used to record the blasts.

6.1 Fragmentation

6.1.1 Test field C1078R013

The test area and the conventionally blasted reference area (current practice) were loaded partially mixed and could not be fully separated in the results. Thus, some amount of test area fragments are included in the current practice data. The results are shown in Table 5 and Figure 23. In total, 143 images were analyzed for current practice data and 89 images for test design data. Camera image examples are shown in Appendix 3.

Table 5. Test field C1078R013 fragment sizes.

Blast design	K20 [cm]	K50 [cm]	K80 [cm]	Fragment size <2.5 cm [%]	Fragment size >1.0 m [%]
Current practice	11.7	28.6	51.6	4.0	0.8
Detonator in the middle	10.2	22.7	41.9	4.1	0.3
Change (%)	-13.1	-20.4	-18.8	2.0	-61.6

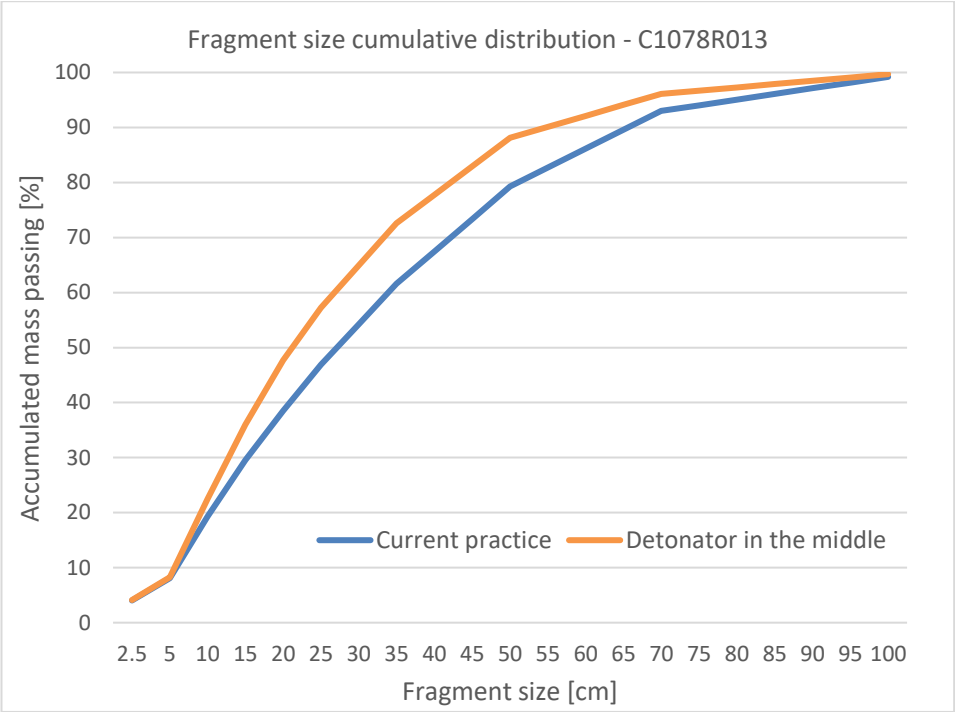

Figure 23. Test field C1078R013 fragment size cumulative distribution.

6.1.2 Test field C1078R011

The test area was divided into three loading blocks (UNW29, UNW30, USW11) and the conventionally charged reference area (current practice) was the loading block UNW28. The loading block with many collapsed holes (UNW27) were left out of the study. The fragment sizes for each studied loading block are shown in Table 6.

Table 6. Test field C1078R011 loading block fragment sizes.

Blast design	Loading block	K20 [cm]	K50 [cm]	K80 [cm]	Fragment size <2.5 cm [%]	Fragment size >1.0 m [%]
Current practice	UNW28	13.2	30.4	56.2	3.3	1.8
Detonator in the middle	UNW30	12.4	28.7	55.9	3.5	2.3
Detonator in the middle	USW11	12.8	30.5	57.8	3.5	2.5
Detonator in the middle	UNW29	13.2	31.8	62.8	3.2	4.4

As we can see, the fragmentation is worst at the loading block UNW29. The block was next to the permanent pit wall, most of the holes were left unstemmed and the bench surface close to the pit wall was more than 1.5m above the target elevation, also one short hole and one collapsed hole was in this relatively small block. Thus, the block was left out of the results shown in Table 7 and Figure 24. Loading block USW11 in the test area included three collapsed holes. The muckpile front in the test area was loaded with rig without machine vision camera, thus fractured area near the bench face producing usually

large size fragments was not in the data. In total, 328 images were analyzed for current practice data and 141 images for test design data. Camera image examples are shown in Appendix 4.

Table 7. Test field C1078R011 fragment sizes.

Blast design	K20 [cm]	K50 [cm]	K80 [cm]	Fragment size <2.5 cm [%]	Fragment size >1.0 m [%]
Current practice	13.2	30.4	56.2	6.7	1.8
Detonator in the middle	12.6	29.6	56.9	7.0	2.4
Change (%)	-4.5	-2.5	1.2	4.6	32.8

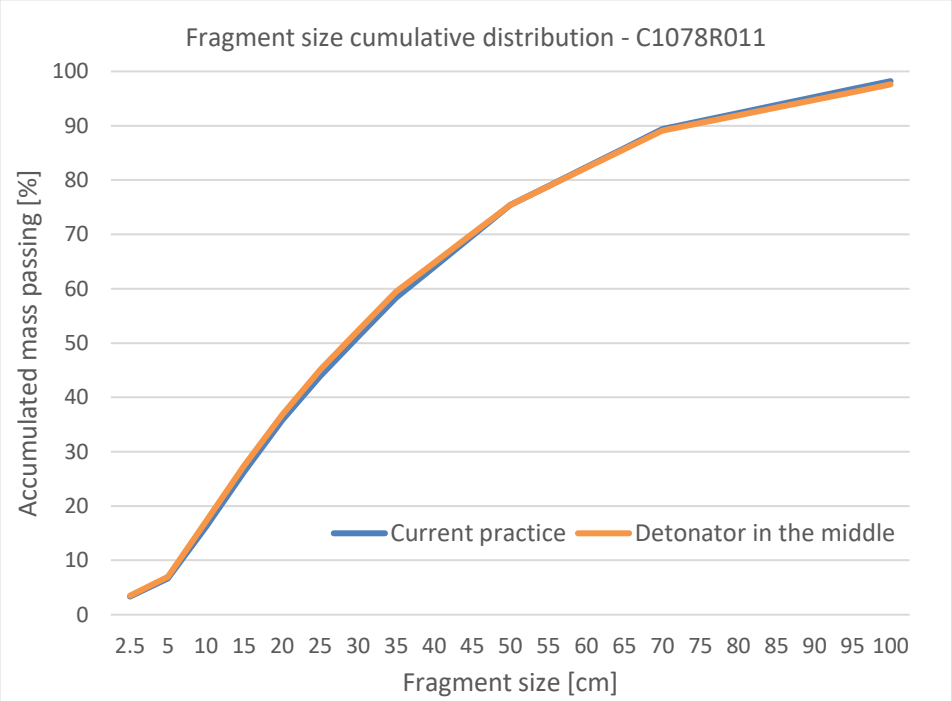

Figure 24. Test field C1078R011 fragment size cumulative distribution.

6.1.3 Test field C1066M003

The test area vas divided into three loading blocks (HG75, HG76, HG77) and the conventionally charged reference area (current practice) was divided into two loading blocks (HG73, HG74). The loading blocks with many collapsed holes and fracture zones (HG78, HG79) were left out of the study. The fragment sizes for each studied loading block are shown in Table 8.

Table 8. Test field C1066M003 loading block fragment sizes.

Blast design	Loading block	K20 [cm]	K50 [cm]	K80 [cm]	Fragment size <2.5 cm [%]	Fragment size >1.0 m [%]
Current practice	HG73	13.9	30.5	55.9	2.7	2.0
Current practice	HG74	14.0	31.0	55.8	2.6	2.0
Detonator in the middle	HG75	14.2	31.8	61.2	2.7	3.9
Detonator in the middle	HG76	11.8	26.1	49.2	3.8	1.1
Detonator in the middle	HG77	12.2	26.4	50.3	3.3	1.7

As we can see, the fragmentation is worst at the loading block HG75. There were two fracture zones, short holes and collapsed hole in this loading block. Thus, the block was left out of the results shown in Table 9 and Figure 25. In total, 562 images were analyzed for current practice data and 277 images for test design data. In ore blasting, the amount of small size fragments in important. Figure 26 shows the result in logarithmic scale so the detonator position effect on small fragments can be seen much better. Camera image examples are shown in Appendix 5.

Table 9. Test field C1066M003 fragment sizes.

Blast design	K20 [cm]	K50 [cm]	K80 [cm]	Fragment size <2.5 cm [%]	Fragment size >1.0 m [%]
Current practice	14.0	30.7	55.9	2.7	2.0
Detonator in the middle	12.0	26.3	49.8	3.5	1.4
Change (%)	-14.1	-14.6	-10.9	30.5	-28.3

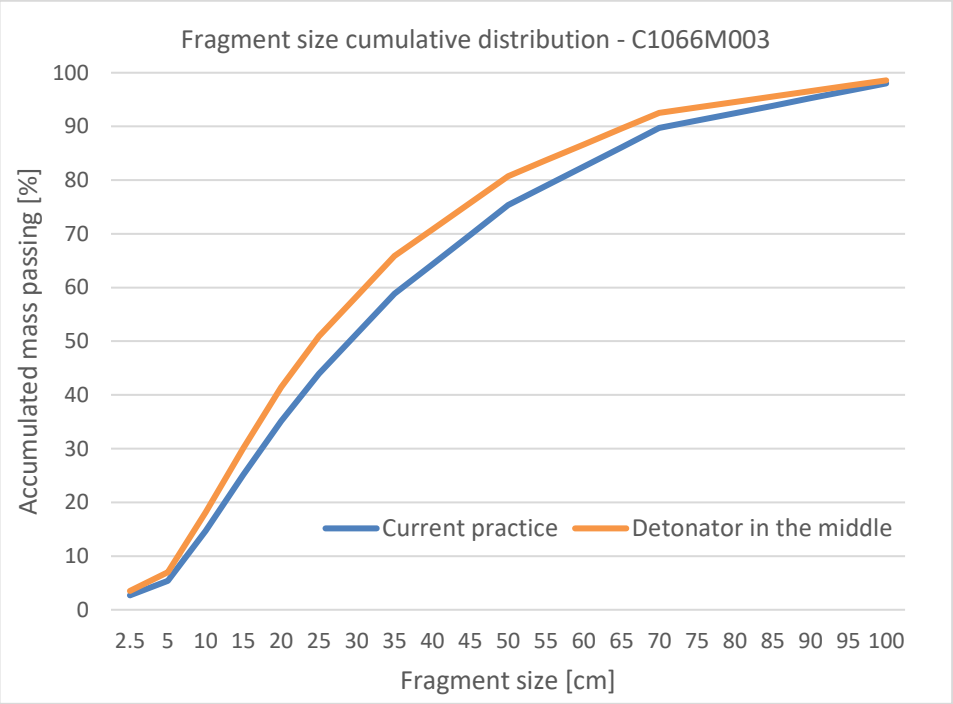

Figure 25. Test field C1066M003 fragment size cumulative distribution.

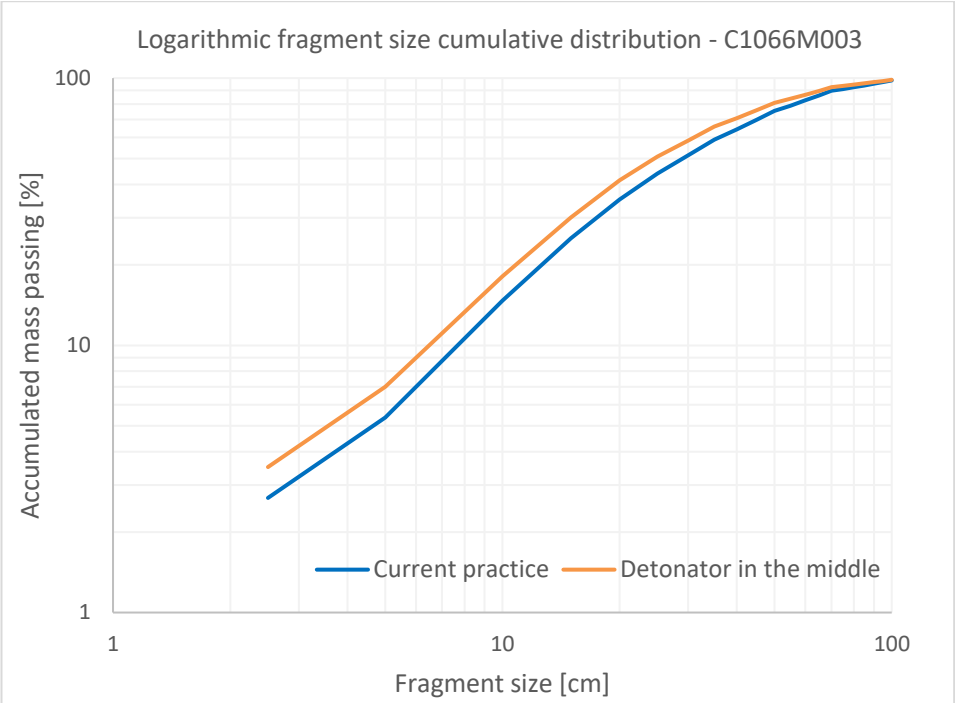

Figure 26. Test field C1066M003 logarithmic fragment size cumulative distribution.

6.2 Loading machine operator feedback

In the test field C1078R013 the loading machine operator feedback forms were filled covering the entire 12 hour shifts, when the loaders were operating on both sides of the test field (in the conventionally blasted reference area and in the test area). In addition, a ramp next to the field was loaded simultaneously. Thus, separation and comparison between the areas based on forms was not possible.

Despite the requests, feedback forms from the test fields C1078R011 and C1066M003 were not filled covering the entire study areas. Thus, comparison based on operator feedback was not possible. A summary of the operator feedback is shown in Appendix 6.

6.3 Loose rock layer below the blast field

Loose rock layer below the blasted field was determined in test field C1066M003 by test drillings. The results were collected using drill automation data by defining the loose rock layer based on the penetration rate of the down-to-hole drills. Generally, penetration rates greater than 0.9 m/min have interpreted as loose rock drilling. The accuracy of the automatic data was 0.5 m. Besides this, the drill rig operators made their own estimate of the thickness of the loose rock layer.

The results are shown in Table 10. The target loading elevation is ±50 cm from the bench floor level. The current practice area was loaded 34 cm below and the test area 43 cm above the target elevation, in average. The test drill holes were planned in the locations between the production blasthole bottoms and the problematic areas (e.g. fracture zones and collapsed holes) were avoided.

Table 10. Loose rock layer test drillings.

Blast design	Drill hole ID	Loading elevation	Difference to targed level [m]	Loose rock layer below the target elevation [m] (Automatic data)	Loose rock layer below the target elevation [m] (Drill rig operators)
Current practice	A9	65.67	-0.33	1.76	0.65
	A10	65.68	-0.32	1.81	1.40
	A11	65.34	-0.66	2.03	1.68
	A12	65.68	-0.32	1.46	1.07
	A13	65.60	-0.40	1.88	1.26
	A14	65.97	-0.03	1.49	1.12
AVG:		65.66	-0.34	1.74	1.20
Test area	A2	66.54	0.54	0.98	0.68
	A4	66.28	0.28	1.71	0.83
	A5	66.52	0.52	0.31	0.88
	A7	66.36	0.36	1.70	1.14
AVG:		66.43	0.43	1.18	0.88

6.4 Assessment of the field test results

Altogether three test fields were blasted. Uncertainties effecting on fragment size, such as fracture zones, collapsed, short or unstemmed holes, were sought to be excluded from the results. All other parameters (e.g. powder factor, muckpile movement direction, blast pattern, hole size) were kept constant on the test and conventionally charged reference area, so that the only variable parameter was the detonator position and geological factors. In the test areas, the detonators were lifted 4 – 5 m above the blasthole bottoms, thus placed in the middle of the explosive column, and in the reference area the detonators were placed, as current practice in Kevitsa, 1 – 1.5 m above the blasthole bottoms.

In the test field C1078R013, the test and reference area were loaded partially mixed and could not be fully separated in the results. The fragment sizes were clearly smaller at the test area (K20 -13.1%, K50 -20.4%, and K80 -18.8%). The amount of small size

fragments (< 2.5 cm) increased 2% and the amount of large size fragments (> 100 cm) reduced 61.6% when the detonators were placed in the middle of the explosive column.

There were four collapsed holes near the bench face in the reference area and a fracture zone pierced the test area. The collapsed holed near the bench faces are usually due to damaged zone (blast damage) from the previous blast, which is very common in Kevitsa. This damaged zone makes the fragmentation worse near the bench faces. According to a borehole pressure measurements conducted in Kevitsa, the initiation of an explosive in this region is sometimes due to previously initiated adjacent hole, meaning that the holes are fired almost simultaneously.

The test field C1078R011 was far from optimal and contained many uncertainties that affected the data. The field was also above the catch bench, no subdrilling was used, and the emulsion column height was shorter than usual, so the middle detonator position effect on fragmentation was expected to be smaller due to smaller difference in stress distribution, detonation time, and rock confinement.

The fragment sizes were smaller in the test area up to K50 and slightly higher with the fragments sizes > K50 (K20 -4.5%, K50 -2.5%, and K80 1.2%). The amount of small size fragments (< 2.5 cm) increased 4.6% and the amount of large size fragments (> 100 cm) increased 32.8% when the detonators were placed in the middle of the explosive column.

The relatively high percentage of collapsed holes in the test area results in larger fragment size. The muckpile front region was loaded with a rig without a machine vision camera, thus, large size fragments from the bench face region in the test area had no effect on the data. It was also found that mounting the detonators during the emulsion pumping by pulling the signal tube (in the test area) was not the best practice; Mounting to the exact location was difficult, mounting was time consuming, and water-emulsion mixtures in the blastholes in the test area are likely. Thus, the result of this test field is not reliable.

In the test field C1066M003, the fragment sizes were clearly smaller in the test area (K20 -14.1%, K50 -14.6%, and K80 -10.9%). The amount of small size fragments (< 2.5 cm) increased 30.5% and the amount of large size fragments (> 100 cm) reduced 28.3% when the detonators were placed in the middle of the explosive column.

There were fracture zones piercing the test area, and based on the slow motion video recorded from the blast, the gas escape from the test area was great. In addition, the field surface was not loaded to the target elevation and the height of the blasted rock mass was approximately 75 cm greater in the test area compared to the reference area. Thus, the quantity of explosive used per cubic of rock blasted (powder factor) was relatively lower. Presumably, the effect of detonator position on fragmentation is greater than the results indicate.

In ore blasting, the small size fragments are important and reduce the energy consumption in grinding. The increased amount of small size fragments in all test areas indicates that the energy used in producing new surfaces of fragments (fragmentation energy) is higher by placing the detonator in the middle of the explosive column.

The feedback received through loading machine operator feedback forms from each test field was not enough to define any difference between the test and reference area. Very generally, loading operators define large size fragments as boulders, although secondary blasting is not needed. The forms were not filled covering the entire study areas, and the impact of changing operators on the results is great. Therefore, this data collection method is no longer recommended.

According to the drill automation data the loose rock layer below the blasted test field C1066M003 was 0.56 m thinner in the test area, in average, and the drill rig operators estimated 0.32 m thinner loose rock layer, compared to the reference area. The accuracy of the automatic data is 0.5 m, but the result is more reliable. In the test area, the detonators were placed about 4 m higher than in the reference area. With 1.5 m subdrilling, the current blasting practice creates 1.74 m, and test design 1.18 m loose rock layer below the bench floor level, in average. Although the number of test drills was small, the result indicated that the thickness of the loose rock layer decreases by placing the detonator in the middle of the explosive column.

Based on the blast videos, the current 3.5 m stemming length used in Kevitsa may not be enough. It looks like the current 1.5 m subdrill is too long, or the current detonator position causes too much damage to the rock mass below the bench floor level.

7 CONCLUSIONS AND RECOMMENDATIONS

The effect of detonator position on fragmentation and bench floor conditions was studied theoretically and in practice by comparing the current blasting practice in Kevitsa, where the detonator is placed about 1 – 1.5 m above the blasthole bottom, to the detonator position in the middle of the explosive column (theoretical optimum).

The theoretical investigation suggested that by placing the detonators in the middle of the explosive column:

- Fragment size is smaller.
- Problematic loose rock layer is thinner, thus there is possibility to decrease the amount of collapsed and short holes, and further increase the fragmentation and reduce toes / floor humps and boulders.
- Stemming length should be studied in order to achieve the optimal blast result.
- Properly positioned double detonator system, where two detonators in one blast hole are initiated at the same time, has advantage over single detonator system, and should result in better fragmentation.

Other theoretical findings were that:

- Presumably, the VOD of the currently used bulk emulsion explosive is not high enough and it should be at least 6868 m/s, which is the average rock mass P-wave velocity in Kevitsa. (In the weathered rock mass the P-wave velocity is probably slower, thus the current explosive VOD 5800 m/s in the upper layer blasting may be enough.)
- Stemming material should be studied in order to achieve the optimal blast result.
- Water and / or drilling fluids on the bottom of the blastholes are problematic and reduce the shock pressure at the water / drilling fluid – explosive interface.
- Rock – explosive interface at the blasthole bottom increases the shock pressure at the interface.

With SHBP-tests and analyzing the old fragment size data it was found out that the amphibole content of the rock has no correlation with the rock UCS and the fragment size in blasting.

The practical investigation showed that by placing the detonators in the middle of the explosive column:

- Fragment sizes (e.g. K20, K50, and K80) can be significantly reduced.
- Amount of small size fragments can be significantly increased.
- Amount of large size fragments can be significantly decreased.
- Thickness of the loose rock layer can be reduced.

Other practical findings were that:

- Current 3.5 m stemming length may not be proper enough.
- Current 1.5 m subdrill is too long, or the current detonator position causes too much damage to the rock mass below the bench floor level.
- Causes for poor bench floor diggability and toes / floor humps are the collapsed or short holes that are mainly due to thick loose rock layer.

I recommend that:

- Tests with the middle detonator position will be continued, and the tests are extended to the double-detonator (electronic detonator) blast fields.
- Effect on fragment size, boulders, and bench floor conditions are monitored.
- Effect on mill throughput and ore recovery are included in the study.
- Possible explosive failures are monitored (a properly positioned double-detonator system and shock wave collision may cause the current blast pattern in ore blasts to be modified).
- Stemming length is studied and adjusted according to the results.
- Proper stemming material is studied.
- Scientific design is used to optimize other blasting related parameters, such as, burden and spacing, delay times, subdrill, and inclination of the blastholes in Kevitsa.

8 SUMMARY

The purpose of this thesis was to study the effect of detonator position on fragmentation theoretically and in practice by changing the position of a detonator near the theoretical optimum (defined by the stress wave theory) and comparing it with the current blasting practice used in Kevitsa mine. The work included the theoretical background study and the effect of rock amphibole content on blasting was determined.

Blasting science was initiated more than 50 years ago, and today it is quite well known that fragmentation is mainly due to blast induced stress waves travelling through the rock mass (without neglecting the effects of gas expansion). Stress waves can be easily measured and modeled, thus scientific design using the stress wave theory allows for significant improvement in rock blasting.

Blasting is the most energy-efficient and cost-effective method to break rock masses. The size of the fragments is an important factor in determining the effectiveness of the blasting and has a major impact on the overall economy of the mine. Rock fragmentation depends mainly on total energy used in fragmentation and stress distribution in the rock mass. The energy released by the explosive is converted into various forms of energy. A detonator position in a blasthole affects the utilization of fragmentation energy and the stress (or energy) distribution in the rock mass. Although very little known, it is one of the most important factors influencing the rock fragmentation.

The most important rock and rock mass properties affecting the blast outcome are rock tensile strength, rock fracture toughness, and rock mass discontinuities. The tensile strength of a rock is much smaller than compressive strength, thus rock mass is mainly destroyed due to tensile failure. A blast-induced compressive stress wave reflects back as a tensile wave from open joints and free surfaces.

The velocity of a stress wave front corresponds to the P-wave velocity of the rock mass and the stress wave induced radial cracks propagate much slower in the rock mass than the P-wave. Rock fragmentation has a strong correlation with the explosive VOD, which should always be matched to the P-wave velocity of the rock mass.

A shock wave and shock pressure, acting in the near field of a blasthole, may increase or decrease at the interface depending on the impedance difference of the materials. Thus, the impedance of the materials e.g. stemming is important. Without the stemming, the energy escape through the collar can be up to 50% of the explosive energy.

In the theoretical study, the theoretical optimum of the detonator position was defined considering an optimal rock fragmentation, which is achieved by placing the detonator in the middle of the explosive column. The current blasting practice in Kevitsa, where the detonators are placed 1 – 1.5 m above the blasthole bottom, causes the stress distribution and rock fracture to be more targeted to the bench floor and not to the bench that we aim to fragment. Theoretically, the thick loose rock layer below the bench floor level could be reduced by placing the detonator upper in the emulsion column. Consequently, the toe / floor hump and poor bench floor diggability problems could be reduced as well when there are less loose rock fragments that can fall to the bottom of the blastholes and shorten the desired hole depth, or cause collapsed holes. Thus, the detonator position in the middle of the explosive column would be more favorable not only to the fragmentation but also to reduce the problems.

The detonator position in the middle of the explosive column, compared to the current detonator placement (in a single-detonator system), has following advantages: (1) the stress distribution in the rock mass is better, (2) the energy efficiency is better, (3) the detonation time is shorter i.e. the total energy of the explosive is released to the rock mass faster, (4) the rock confinement is smaller, thus more energy is used for fragmentation and not distributed to the rock mass in the form of seismic energy, (5) the stress wave superposition (i.e. greater stress) is achieved, and (6) the loading rate and kinetic energy of flying fragments may be increased resulting in better fragmentation. Theoretically, by placing the detonator in the middle of the explosive column the stemming length can be reduced and still keep the same amount of energy in the blasthole. Considering that adequate confinement cannot be jeopardized.

A double-detonator system advantages over single-detonator system are (1) more even stress distribution and (2) shock wave collision that creates higher pressure and stress in the surrounding rock mass resulting in better fragmentation.

The practical part of this thesis included three test fields within the production blasts where the effect of detonator position was studied in practice. The test design (detonator

in the middle of the explosive column) was compared to the current practice used in Kevitsa. As a result, fragmentation was significantly improved with the test design. Moreover, the test drillings showed that the thickness of the loose rock layer below the blasted field decreases with the test design. However, the number of the test drills was small and more study is needed.

The SHPB tests showed that there is no correlation between dynamic rock strength and rock amphibole content, and analysis of old fragment size data showed that amphibole content is not relevant for fragment size in blasting.

Overall, this study indicates that the scientific design based on the stress wave theory has potential to improve rock blasting and that detonator position has significant impact on fragmentation in open pit blasting.

REFERENCES

Awuah-Offei K. (ed.), 2018. Energy Efficiency in the Mineral Industry. Springer International Publishing, 333 p. ISBN 978-3-319-54198-3

Bergman P., 2005. Optimisation of Fragmentation and Comminution at Boliden Mineral, Aitik Operation. Licentiate thesis, Luleå University of Technology, Luleå.

Bergström P., 2017. Drill and Blast operations at the Kevitsa mine. Lecture notes, University of Oulu, Oulu Mining School, delivered 4 December 2017.

Beyglou A., Schunnesson H., Johansson D. & Johansson N., 2015. Adjusting Initiation Direction to Domains of Rock Mass Discontinuities in Aitik Open Pit Mine. 11th International Symposium on Rock Fragmentation by Blasting, Sydney.

Boylston A., 2018. How to ensure energy efficiency in mining 1/4: Comminution circuit design [online document]. Helsinki: Metso. Available from: https://www.metso.com/blog/mining/how-to-ensure-energy-efficiency-in-mining-part-one [Accessed 31 December 2019].

Brinkmann J.R. An experimental study of the effects of shock and gas penetration in blasting. In: Proceedings of 3th International Symposium on Rock Fragmentation by Blasting, p. 55-66.

Brunton I.D., Fraser S.J., Hodgkinson J.H. & Stewart P.C., 2010. Parameters influencing full scale sublevel caving material recovery at the Ridgeway gold mine. International Journal of Rock Mechanics and Mining Sciences, 47, p. 674-656.

Chen B.B., Liu C.Y., & Yang J.X., 2018. Design and Application of Blasting Parameters for Presplitting Hard Roof with the Aid of Empty-Hole Effect. Shock and Vibration, Vol. 2018, Article ID 8749415. Available from: https://doi.org/10.1155/2018/8749415 [Accessed 2 December 2019].

Cho S.H. & Kaneko K., 2004. Rock Fragmentation Control in Blasting. Materials Transactions, 45, p. 1722-1730. Available from: https://www.jim.or.jp/journal/e/pdf3/45/05/1722.pdf [Accessed 23 December 2019].

Cooper P.W., 1996. Explosives engineering. New York: Wiley-VCH, 480 p. ISBN: 978-0471186366

Gercek H., 2007. Poisson's ratio values for rocks. International Journal of Rock Mechanics and Mining Sciences, 44, p. 1-13. doi: 10.1016/j.ijrmms.2006.04.011

Howe S. & Pan J., 2018. Application of Enterprise Optimisation Considering Ultra High Intensity Blasting Strategies. Whittle Consulting Pty Ltd. Available from: https://www.whittleconsulting.com.au/wp-content/uploads/2018/04/Application-of-EO-Considering-Ultra-High-Intensity-Blasting-Strategies.pdf [Accessed 2 January 2020].

Jeswiet J. & Szekeres A., 2016. Energy Consumption in Mining Comminution. Procedia CIRP, 48, p.140-145.

Jimeno C.L., Jimeno E.L. & Carcedo F.J.A., 1995. Drilling and blasting of rocks. Rotterdam: CRC Press, 408 p. ISBN 978-9054101994

Konya C.J. & Konya A., 2018. Effect of Hole Stemming Practices on Energy Efficiency of Comminution. In: Awuah-Offei K. (ed.) Energy Efficiency in the Mineral Industry. Springer International Publishing, p. 31-53. ISBN 978-3-319-54198-3

Konya C.J. & Walter E.J., 1990. Surface Blast Design. New Jersey: Prentice Hall, 303 p. ISBN: 978-0138779948

Makkonen H., Halkoaho T., Konnunaho J., Rasilainen K., Kontinen A. & Eilu P., 2017. Ni-(Cu-PGE) deposits in Finland - Geology and exploration potential. Ore Geology Reviews. doi: 10.1016/j.oregeorev.2017.06.008

Małkowski P., Ostrowski Ł. & Brodny J., 2018. Analysis of Young's modulus for Carboniferous sedimentary rocks and its relationship with uniaxial compressive strength usinf different methods of modulus determination. Journal of Sustainable Mining, 17, p. 145-157.

Menacer K., Hafsaoui A., Talhi K. & Saadoune A., 2015. Study of the Influence Factors on Rock Blasting. In: WMESS. (ed.) Procedia Earth and Planetary Science, 15, p. 900-907. doi: 10.1016/j.proeps.2015.08.143

Mishra A., Rout M., Singh D.R. & Jana S., 2017. Influence of density of emulsion explosives on its velocity of detonation and fragmentation of blasted muckpile. Current Science, 112, p. 602-608. doi: 10.18520/cs/v112/i03/602-608

Mozie K.N., 2017. Characterization of Ultrasonic Waves in Various Drilling Fluids [Master's thesis]. University College of Southeast Norway.

Natural Resources Conservation Service (USDA), 2012. Engineering Classification of Rock Materials. In: National Engineering Handbook, 210-VI, Part 631, Chapter 4. U.S. Department of Agriculture. 61 p.

Orica Technical Services, 1998. Safe and Efficient Blasting in Open Cut Mines. Orica Australia Pty Ltd.

Otuonye F.O., 1981. Effetive Blasthole Stemming. (Doctoral dissertation) Ohio State University, US, 191 p.

Parra Galvez H., 2013. Blast induced fragment conditioning and its effect on impact breakage and leaching performance. (Doctoral dissertation) University of Queensland, Australia, 295 p.

Petropoulos N., Beyglou A., Johansson D., Nyberg U. & Novikov E., 2014. Fragmentation by Blasting through Precise Initiation: Full Scale Trials at the Aitik Copper Mine. Blasting and Fragmentation, 8, p. 87-100.

Read J. & Stacey P. (eds.), 2009. Guidelines for open pit slope design. Australia: CSIRO Publishing, 496 p. ISBN 9780415874410

Prasad S., Choudhary B.S. & Mishra A.K., 2017. Effect of Stemming to Burden Ratio and Powder Factor on Blast Induced Rock Fragmentation – A Case Study. In: IOP Conference Series: Materials Science and Engineering, 225. doi: 10.1088/1757-899X/225/1/012191

Sanchidrián J.A., Pablo S. & López L.M., 2007. Energy components in rock blasting. International Journal of Rock Mechanics and Mining Sciences, 44, p. 130-147. doi: 10.1016/j.ijrmms.2006.04.011

Silva J., Worsey T., & Lusk B., 2019. Practical assessment of rock damage due to blasting. International Journal of Mining Science and Technology, 29, p. 379-385. Available from: https://www.sciencedirect.com/science/article/pii/S2095268617306158 [Accessed 19 December 2019].

Singh S.P. & Narendrula R., 2010. Causes, implications and control of oversize during blasting. In: Sanchidrián J.A. (ed.) Rock Fragmentation by Blasting: Proceedings of the 9th International Symposium on Rock Fragmentation by Blasting. London: Taylor & Francis Group, 872 p. ISBN 978-0-415-48296-7

Yi C.P., Johansson D., Schunnesson H. & Åhlin H., 2019. Numerical study of the impact of joints on rock fragmentation by blasting. In: Holmberg R. et al. (eds.) 10th EFEE World Conference on Explosives and Blasting. UK: European Federation of Explosives Engineers, p. 289-307. ISBN 978-0-9550290-6-6

Zaid A.I.O., 2016. Stress Waves in Solids, Transmission, Reflection and Interaction and Fractures Caused by Them: State of the Art. International Journal of Theoretical and Applied Mechanics, 1, p. 155-164.

Zhang Z.X., Kou S.Q., Jiang L.G. & Lindqvist P.A., 2000. Effects of loading rates on rock fracture: Fracture characteristics and energy partitioning. International Journal of Rock Mechanics and Mining Sciences, 37, p. 745-762.

Zhang Z.X., 2002. An empirical relation between Mode I fracture toughness and tensile strength of rock. International Journal of Rock Mechanics and Mining Sciences, 39, p. 401-406.

Zhang Z.X., 2005. Increasing ore extraction by changing detonator positions in LKAB Malmberget mine. Fragblast, 9, p. 29-46.

Zhang Z.X. & Naarttijärvi T., 2006. Applying fundamental principles of stress waves to production blasting in LKAB Malmberget mine. In: Proceedings of 8th International Symposium on Rock Fragmentation by Blasting, p. 369-374.

Zhang Z.X., 2008. Impact of rock blasting on mining engineering. In: Proceedings of 5th International Conference & Exhibition on Mass Mining, p. 671-680. Available from: https://www.researchgate.net/publication/315728893_Impact_of_rock_blasting_on_mining_engineering [Accessed 20 November 2019].

Zhang Z.X., 2014. Effect of double-primer placement on rock fracture and ore recovery. International Journal of Rock Mechanics and Mining Sciences, 71, p. 208-216.

Zhang Z.X., 2016. Rock fracture and blasting – Theory and applications. Oxford: Elsevier Science, 505 p. ISBN 978-0-12-802668-5

Zhang Z.X., 2017. Kinetic energy and its applications in mining engineering. International Journal of Mining Science and Technology, 27, p. 237-244.

Zhang Z.X., 2019. Challenges and potentialities of rock blasting in mining engineering. Materia, 5, p. 19-22.

Appendix 1. Ore blocks used in fragment size vs amphibole content comparison.

Ore block ID	Explosive	Diameter [mm]	Pattern [m x m]	Amphibole content [%]	K20 [cm]	K50 [cm]	K80 [cm]
B1090X022-HG47	Fortis Extra	225	4.4 x 5.2	10.7	12.93	29.03	53.52
B1102X006-HG12	Fortis Extra	225	4.4 x 5.2	16.2	10.78	24.87	45.51
B1102X006-HG11	Fortis Extra	225	4.4 x 5.2	16.4	6.42	14.16	23.86
			AVG:	14.4	10.0	22.7	41.0
B1090X021-HG44	Fortis Extra	225	4.4 x 5.2	18.7	8.40	18.13	32.34
B1090X022-HG48	Fortis Extra	225	4.4 x 5.2	21.1	11.91	25.35	44.15
B1090X021-HG43	Fortis Extra	225	4.4 x 5.2	22.0	8.73	21.01	40.48
B1090X020-HG38	Fortis Extra	225	4.4 x 5.2	23.0	10.60	22.83	40.54
			AVG:	21.2	9.9	21.8	39.4
B1102X006-HG9	Fortis Extra	225	4.4 x 5.2	24.2	11.48	25.61	45.15
B1102X006-HG10	Fortis Extra	225	4.4 x 5.2	25.7	9.62	19.68	32.71
B1090X022-HG46	Fortis Extra	225	4.4 x 5.2	26.1	8.86	21.25	40.73
B1090X020-HG42	Fortis Extra	225	4.4 x 5.2	26.7	13.60	29.38	50.03
			AVG:	25.7	10.9	24.0	42.2
B1090X021-HG45	Fortis Extra	225	4.4 x 5.2	27.7	11.42	26.22	47.26
B1102X006-HG14	Fortis Extra	225	4.4 x 5.2	28.2	10.37	23.29	42.64
B1126X012-HG7	Fortis Extra	225	4.4 x 5.2	30.3	7.77	17.78	33.12
B1114X005-HG10	Fortis Extra	225	4.4 x 5.2	31.7	7.57	17.23	32.36
			AVG:	29.5	9.3	21.1	38.8
B1090X020-HG39	Fortis Extra	225	4.4 x 5.2	35.6	7.03	15.29	27.85
B1102X006-HG13	Fortis Extra	225	4.4 x 5.2	36.7	11.26	25.10	45.63
B1090X020-HG41	Fortis Extra	225	4.4 x 5.2	48.6	8.80	19.75	37.75
B1090X020-HG40	Fortis Extra	225	4.4 x 5.2	54.7	10.35	23.76	43.63
			AVG:	43.9	9.4	21.0	38.7

Appendix 2. Waste rock blocks used in fragment size vs amphibole content comparison.

Waster rock block ID	Explosive	Diameter [mm]	Pattern [m x m]	Amphibole content [%]	K20 [cm]	K50 [cm]	K80 [cm]
B1126R032-UsW19	Fortis Advantage	165	3.8 x 4.4	26.4	10.5	22.7	44.6
B1114X001-UsW2	Fortis Advantage	165	3.8 x 4.4	31.6	10.4	21.8	40.7
B1114R022-UsW11	Fortis Advantage	165	3.8 x 4.4	34.0	9.6	20.0	38.4
			AVG:	30.7	10.2	21.5	41.2
B1114X013-UnW20	Fortis Advantage	165	3.8 x 4.4	34.3	8.5	19.0	34.2
B1114R022-UnW27	Fortis Advantage	165	3.8 x 4.4	37.6	10.9	21.4	37.1
B1114R016-CW5	Fortis Advantage	165	3.8 x 4.4	37.9	10.5	20.9	38.6
			AVG:	36.6	10.0	20.4	36.6
B1126R020-UsW3	Fortis Advantage	165	3.8 x 4.4	38.3	6.5	15.7	31.5
B1126X003-UnW5	Fortis Advantage	165	3.8 x 4.4	38.6	10.1	24.9	50.4
B1114X001-UnW2	Fortis Advantage	165	3.8 x 4.4	39.0	10.7	21.1	37.5
			AVG:	38.7	9.1	20.6	39.8
B1114X026-CW11	Fortis Advantage	165	3.8 x 4.4	39.1	8.9	19.4	37.4
B1126X002-UnW2	Fortis Advantage	165	3.8 x 4.4	40.3	10.9	21.1	40.8
B1126X003-UnW4	Fortis Advantage	165	3.8 x 4.4	44.3	10.2	20.6	39.5
			AVG:	41.2	10.0	20.4	39.2
B1138X033-CW9	Fortis Advantage	165	3.8 x 4.4	45.5	12.1	24.4	45.7
B1126X002-UnW3	Fortis Advantage	165	3.8 x 4.4	46.4	9.0	20.3	37.5
B1126X003-UsW2	Fortis Advantage	165	3.8 x 4.4	48.1	10.4	20.5	37.5
			AVG:	46.7	10.5	21.7	40.2
B1138X033-UnW28	Fortis Advantage	165	3.8 x 4.4	51.3	11.0	24.2	49.1
B1138X033-UnW29	Fortis Advantage	165	3.8 x 4.4	60.2	10.5	21.4	40.0
			AVG:	55.7	10.8	22.8	44.6

Appendix 3. Examples of test field C1078R013 machine vision camera images.

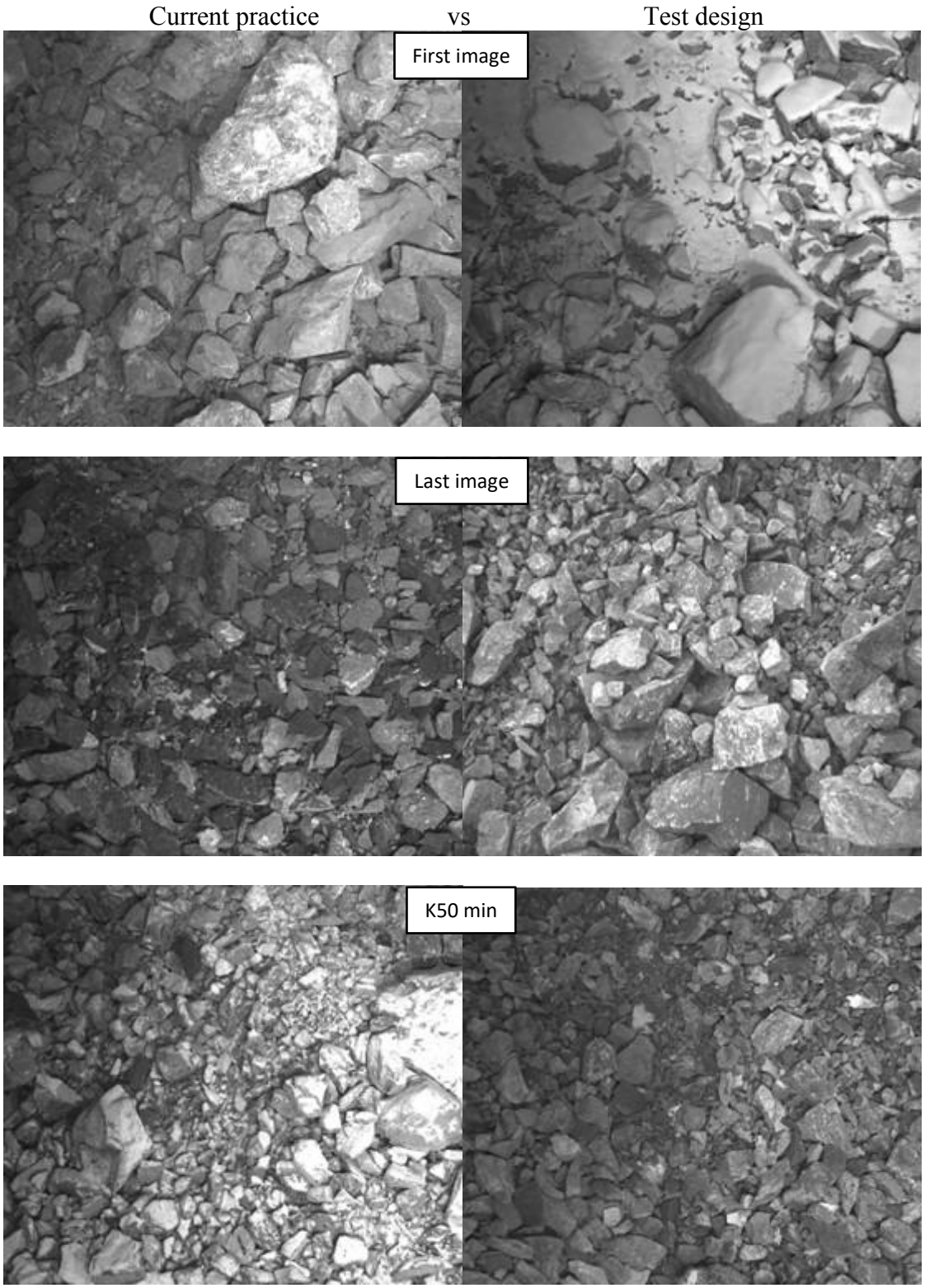

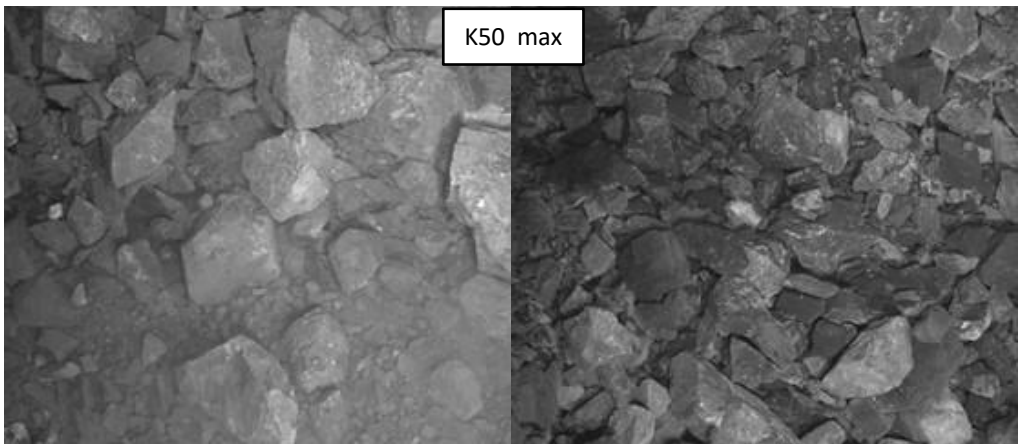
K50 max

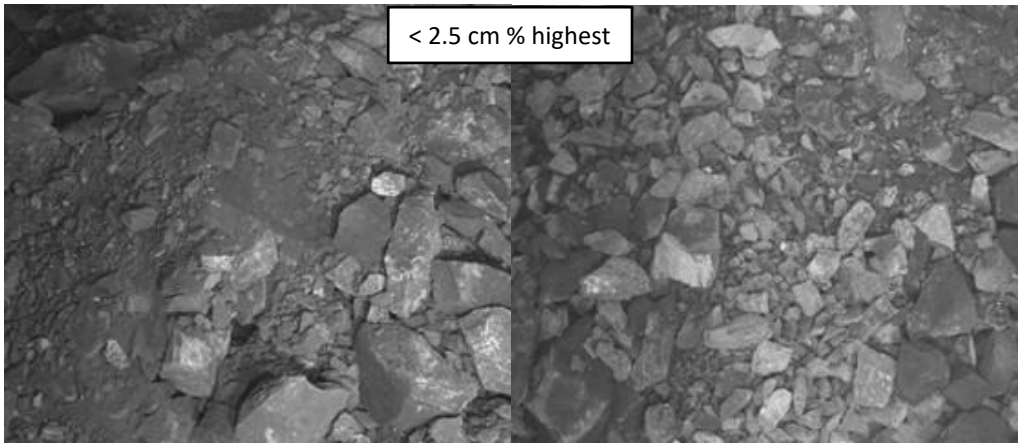
< 2.5 cm % highest

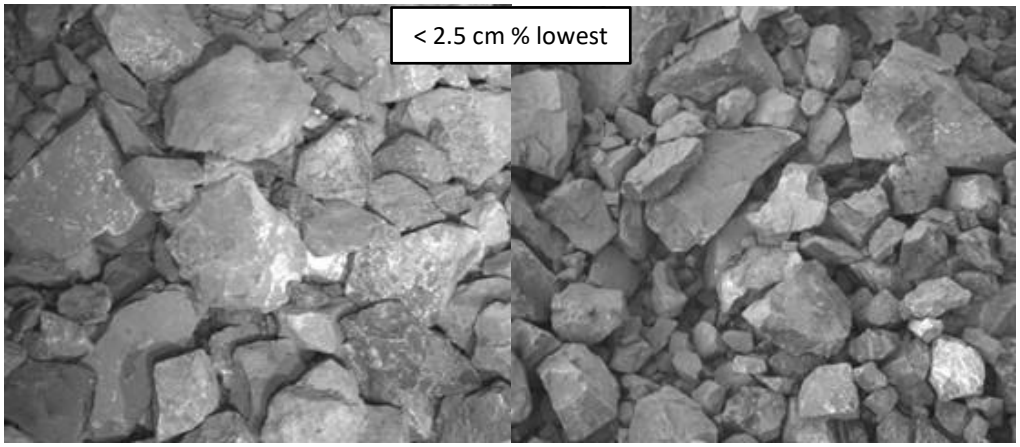
< 2.5 cm % lowest

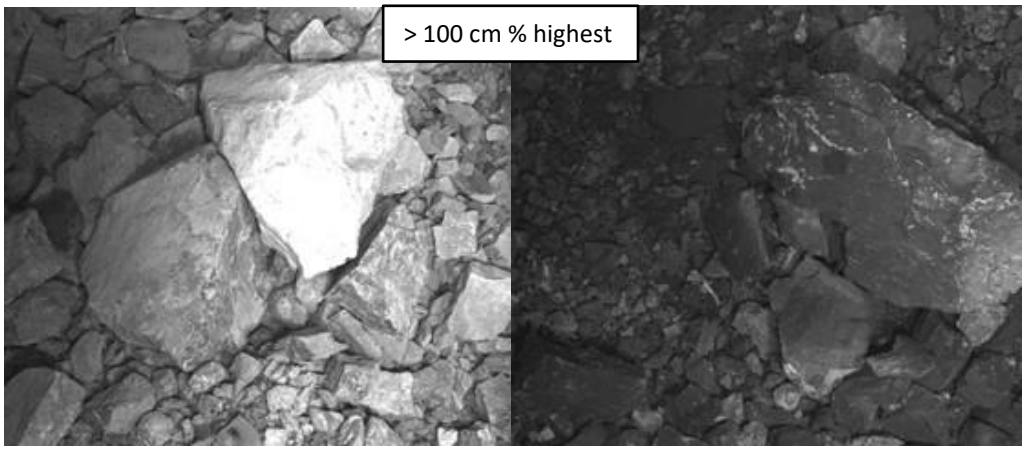
> 100 cm % highest

Appendix 4. Examples of test field C1078R011 machine vision camera images.

Current practice vs Test design

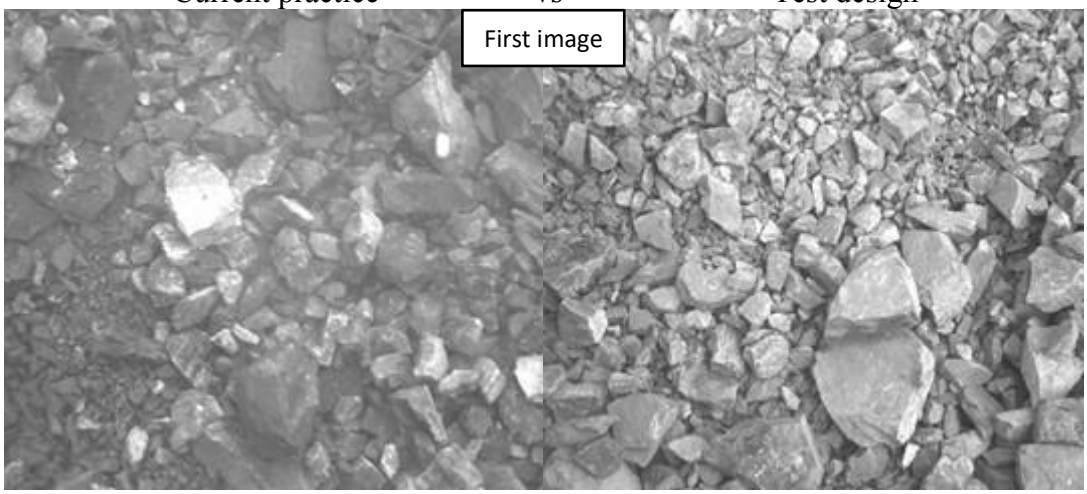

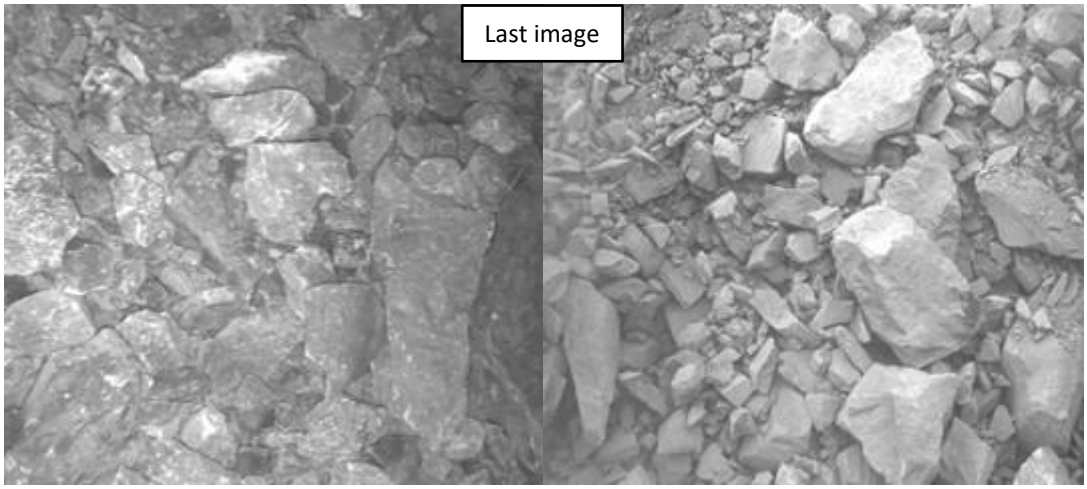

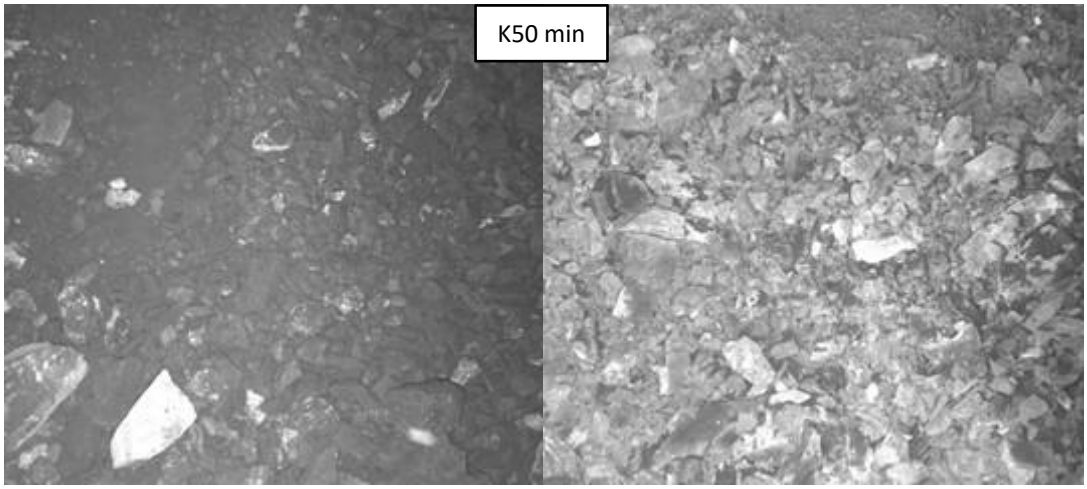

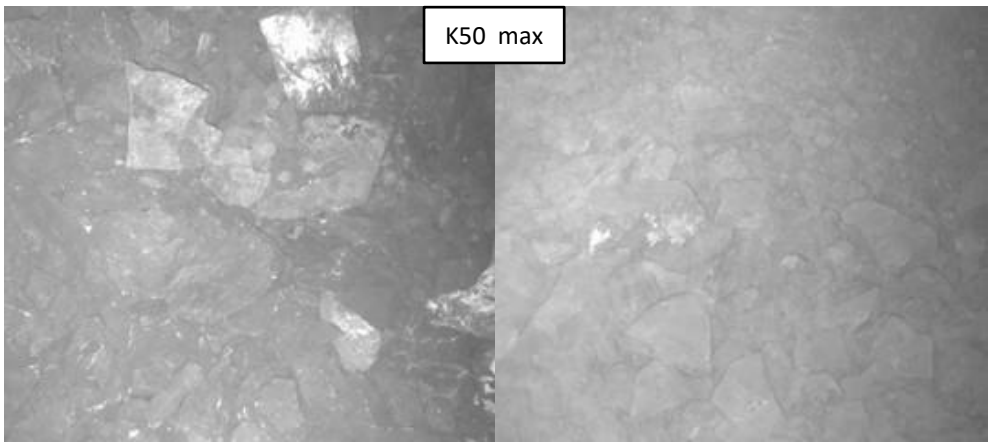
K50 max

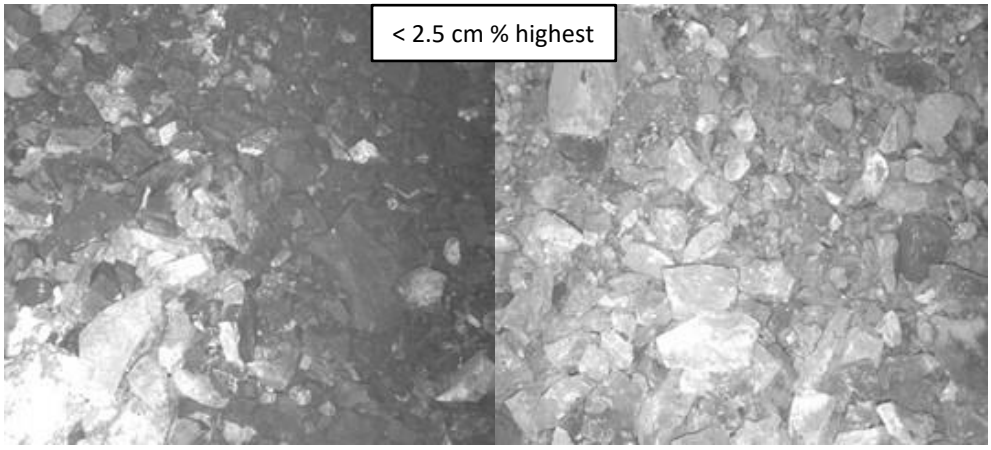
< 2.5 cm % highest

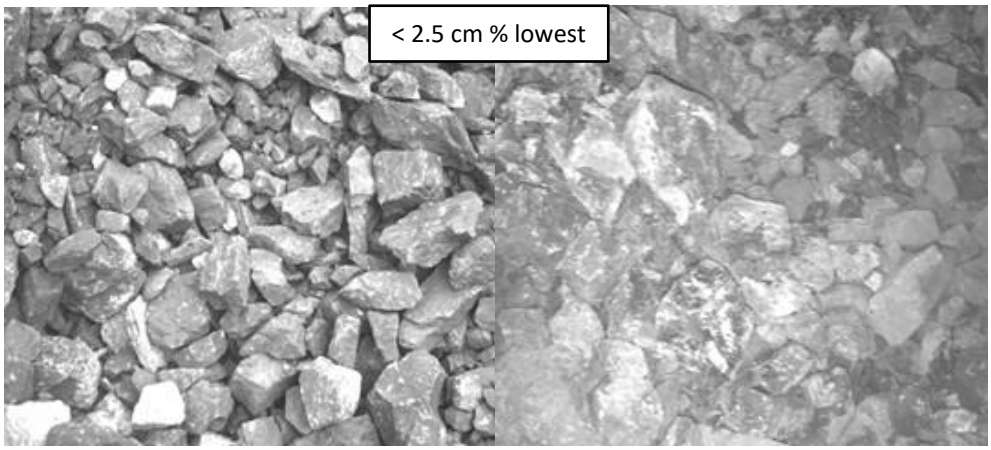
< 2.5 cm % lowest

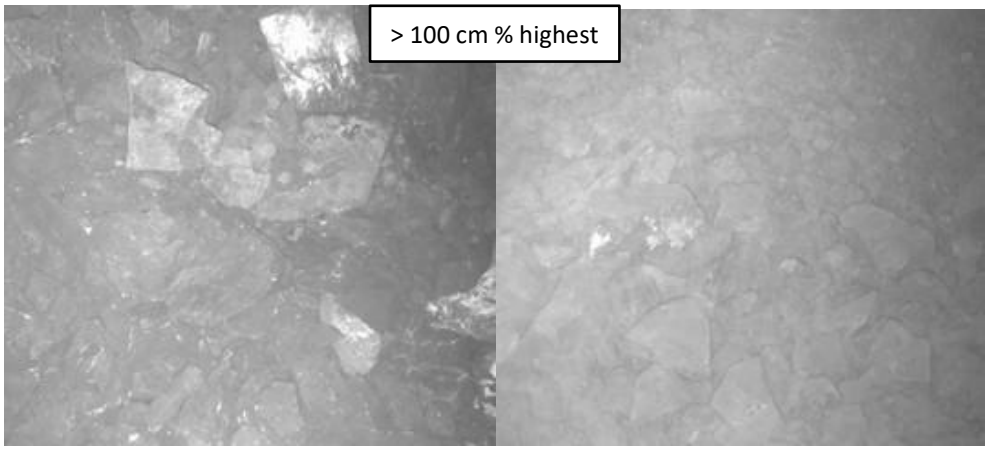
> 100 cm % highest

Appendix 5. Examples of test field C1066M003 machine vision camera images.

Current practice vs Test design

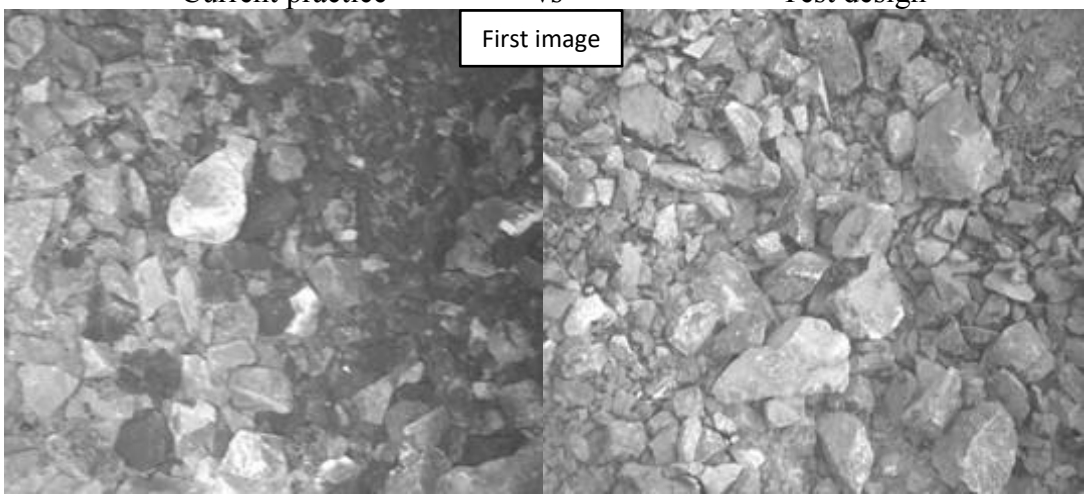

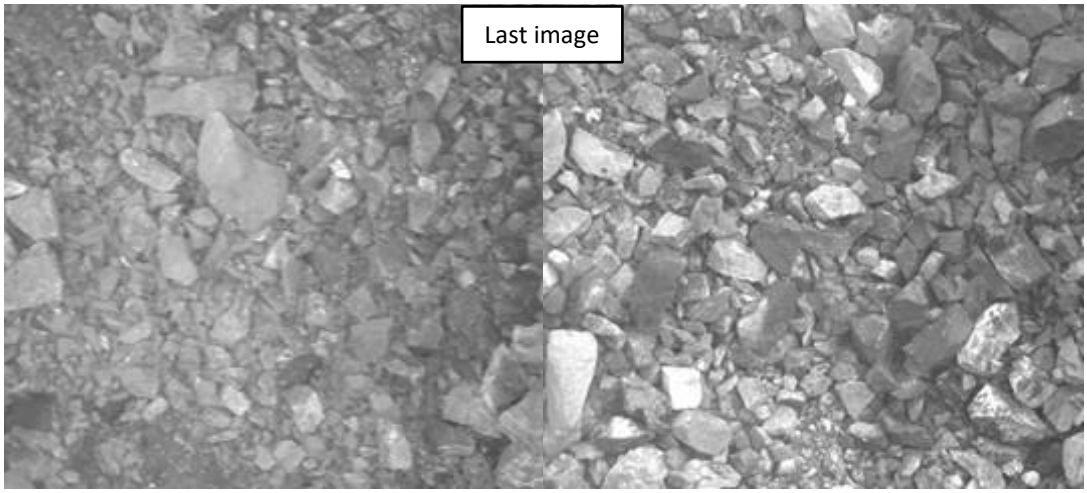

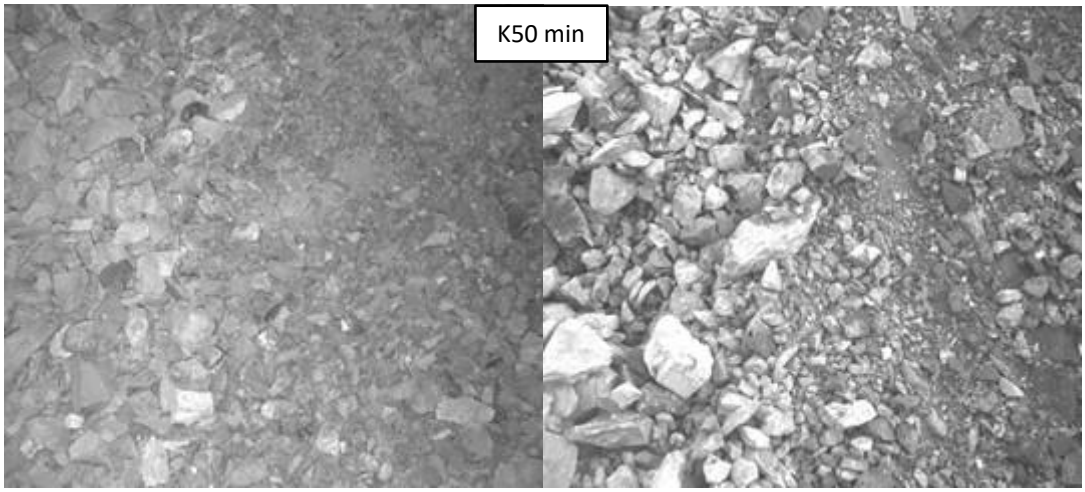

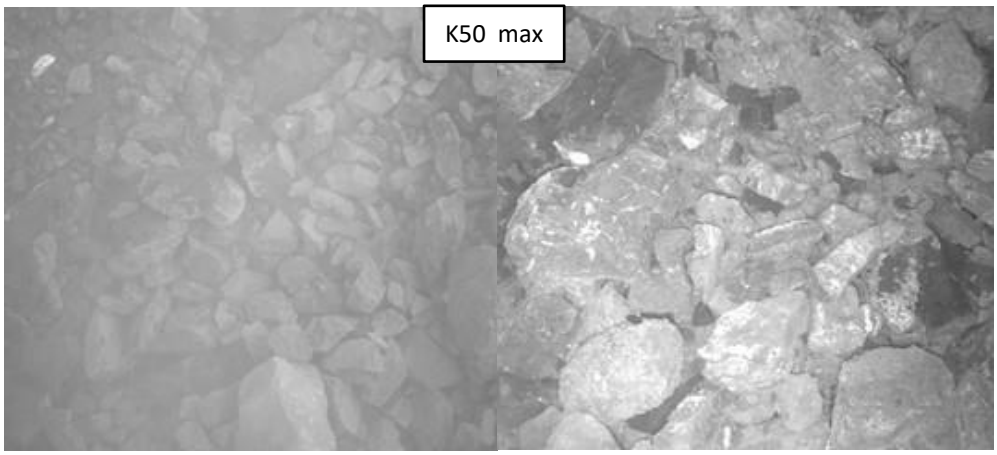
K50 max

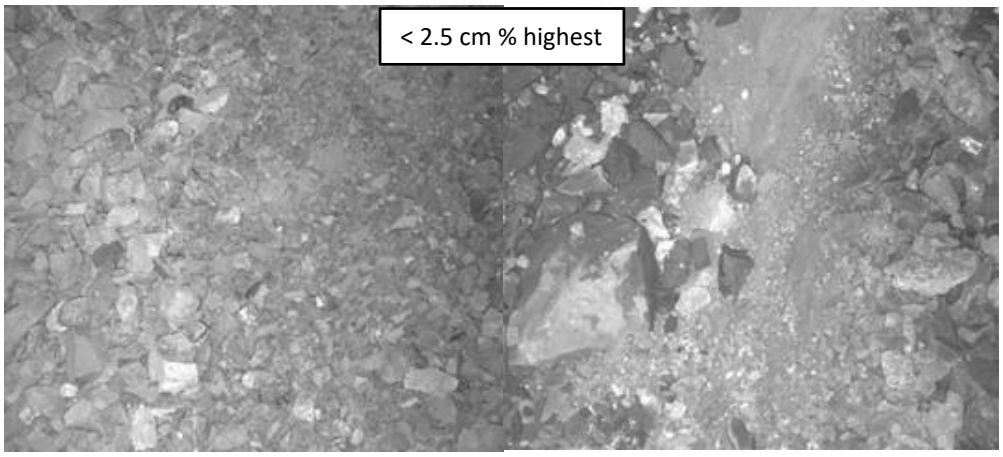
< 2.5 cm % highest

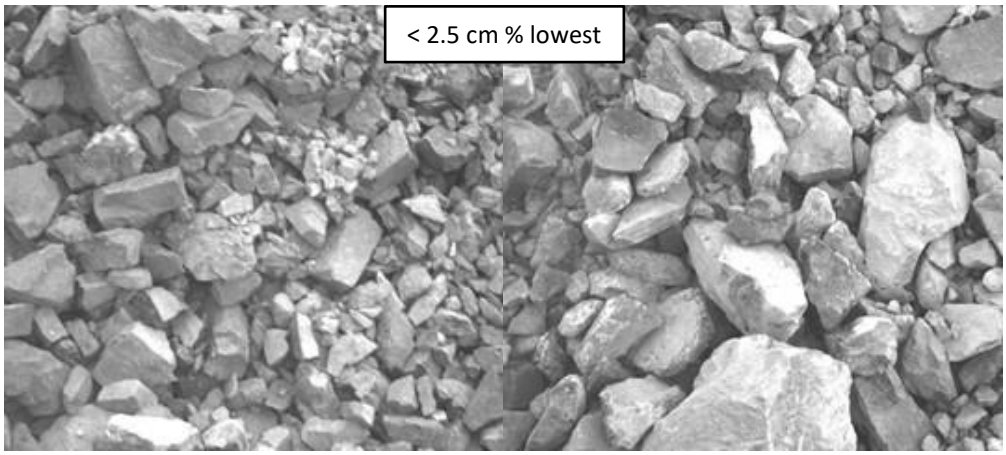
< 2.5 cm % lowest

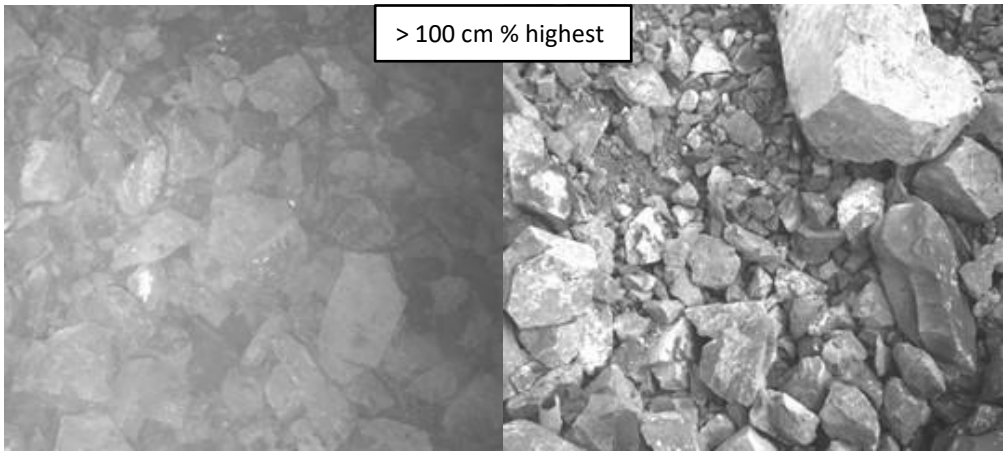
> 100 cm % highest

Appendix 6. Loading machine operator feedback from the test fields.

Table 1. Summary of loading operator feedback from the test field C1078R013.

Loading area	Muckpile diggability (1-5)	Number of boulders	Bench floor condition	Problems	Other comments
Mixture (reference + test area)	4	Few	-	No	Good blast
Mixture (reference + test area + ramp)	3 - 4	5	Stays well on target level	No	Reasonably good blast
Mixture (reference + test area + ramp)	4	-	OK	No	-
Mixture (test area + ramp)	4	10	Coarse	No	A couple of tighter points, drill holes in rocks, rocks had not moved
Ramp	3	-	-	Boulders	-

Table 2. Summary of loading operator feedback from the test field C1078R011.

Loading area	Muckpile diggability (1-5)	Number of boulders	Bench floor condition	Problems	Other comments
UNW28 (reference area)	1	1	Very poor floor and very tight even when loading 1m above the target level	Poor floor + boulders	-
UNW28 (reference area)	2.5	5 - 10	More than 1m above the targed level. I started lowering.	Poor floor + boulders	-
UNW28 (reference area)	3	< 10	Tight	Poor floor	New shovel bucket tooths would help
UNW28 (reference area)	4	3 (moved)	Hard floor, 1m above the targed level	Poor floor	Rock ok
UNW28 (reference area)	3	1	Hard, not able to reach targed level	Poor floor	Rock has not moved in blasting
UNW28 (reference area)	2	0	Only toes	Poor floor	-
UNW28 (reference area)	2	-	Toes	Poor floor	-
Test area	2	-	Tight floor	Boulders	UNW0029 not moved properly in blasting
Test area	3	2 / haul truck	Poor floor, many toes	Poor floor + boulders	-
UNW29 (test area)	1	4	Extremely poor!	Poor floor	-
UNW27 (mixture of reference and test area)	2-3	Only few	Many toes. Clearly can be seen that there was many collapsed holes in the area	Poor floor	Fragment size was relatively small, but tight to load.

Table 3. Summary of loading operator feedback from the test field C1066M003.

Loading area	Muckpile diggability (1-5)	Number of boulders	Bench floor condition	Problems	Other comments
Muckpile front (test area)	2	-	Large boulders tightly in the floor, the upper part was easier to load	Poor floor + boulders	-
Muckpile front (reference + test area)	3	ca. 10	Working on muckpile front, not on the bench floor. Poor diggability.	Boulders	Boulders on top of the bench, otherwise the fragment size was ok
HG78 (reference area)	4	0	Normal / good	No	-